University of Southern Queensland

Faculty of Health, Engineering and Sciences

Improving Caravan Design by Modelling of Crosswind

A dissertation submitted by

Mr Adrian De Leon

in fulfilment of the requirements of

Courses ENG4111 and ENG4112 Research Project

towards the degree of

Bachelor of Engineering (Mechanical Engineering)

Submitted October 2016

ABSTRACT

It is a well-known fact that towing a caravan over long distances can be a very expensive exercise especially with the rise in cost of fuel. Caravans by design are generally not seen to exhibit any standout aerodynamic features and as such can increase the fuel consumption of the tow vehicle by more than double. The effects of wind on the aerodynamics of the caravan are also of importance. Of particular interest, the effect that cross wind flow has on caravans is somewhat of an under stated issue. This project aims to analyze the effect of crosswind flow, propose some caravan modifications and evaluate any advantages to the tow vehicle regarding fuel economy.

The project aims to use Computational Fluid Dynamics to evaluate the caravan under a variety of operating conditions. By conducting a parametric study into various design features on the caravan it is possible to evaluate these proposal with CFD to obtain data that can show the potential increases in efficiency and economy over the original baseline design.

The results show that there are significant forces at play when analyzing crosswind flow on the caravan. The results also show that by carrying out modifications to key areas such as the gap between the car and caravan and also its general shape, there is potential for significant gains to be made in reducing the drag forces at play and subsequently enhancing the fuel economy of the tow vehicle. Results confirm that these forces can be reduced by up to 18%.

University of Southern Queensland

Faculty of Health, Engineering and Sciences

ENG4111/ENG4112 Research Project

LIMITATIONS OF USE

CERTIFICATION OF DISSERTATION

I certify that the ideas, designs, experimental work, results, analyses and conclusions set out in this dissertation are entirely my own effort, except where otherwise indicated and acknowledged.

I further certify that the work is original and has not been previously submitted for assessment in any other course or institution, except where specifically stated.

Adrian De Leon

Student Number: 0050108437

_____

Signature

_____

Date

ACKNOWLEDGEMENTS

TABLE OF CONTENTS

LIST OF FIGURES

LIST OF TABLES

LIST OF APPENDICES

NOMENCLATURE

The following abbreviated terms have been utilized throughout this dissertation.

CFD	Computational Fluid Dynamics
WH&S	Work Health & Safety
km/h	kilometres per Hour
N	Newton's
USQ	University of Southern Queensland
m/s	metres per second
SST	Shear Stress Transport
F	Aerodynamic Load
C_d	Coefficient of Drag
v	Velocity (m/s)
ρ	Air Density (kg/m^3)
A	Frontal Area (m^2)
GRP	Glass Reinforced Plastic

CHAPTER 1 - INTRODUCTION

1.1 Background

Recreational travel using caravans has been embraced by millions worldwide. The industry has grown steadily since the mid to late 1950's and the last two decades have seen an exponential increase in technological advancement which has served to provide travelers with a 'home away from home' which affords the ultimate in creature comforts and flexibility.

Statistics on Recreational Vehicle (RV) usage within Australia as collected by the Australian Bureau of Statistics (ABS) indicates that there are over half a million registered recreational vehicles in use, with 90% of these categorized as caravans or towable camping trailers.

Caravan design has evolved significantly throughout the decades. The focus on improving aerodynamic efficiency has been at the top of many caravan design and manufacturer's priority lists. As caravan designs grow in size and complexity, the performance characteristics of the towing vehicles have also had to improve in order to provide the optimum capability to safely and efficiently tow these caravans.

Significant effort has been made to ensure a caravan's shape and form is optimized to provide maximum aerodynamic efficiency, in order to reduce the environmental and economic impact due to the drag developed as it moves behind the tow vehicle, whilst also ensuring maximum safety in relation to its dynamic stability under the influence of external wind loads.

1.2 Outline of the Study

This study aims to expand on the research conducted by Briskey (2013) in which a tow vehicle and caravan combination was evaluated using computational fluid dynamics (CFD) practices. The study conducted by Briskey (2013) focused on the aerodynamic drag produced by the caravan from a headwind perspective.

This study is primarily concerned with aerodynamic drag produced when the caravan is subject to cross wind air flow and its subsequent effect on the fuel efficiency of the tow vehicle. In addition, initial data gathered as part of this study will form part of an

optimization strategy for the baseline caravan configuration which will aim to reduce the effects of aerodynamic drag on the caravan and enhance lateral stability.

This study will build on and explore the effects of cross wind aerodynamic loading on moving vehicles as encountered throughout a literature review in which the majority of literature focuses on vehicles such as cars, trucks and trains. The research will feature a parametric study conducted on modifications to a baseline caravan geometry such as that depicted in Figure 1, which will be assessed for their ability to reduce drag and therefore make the caravan design more aerodynamically efficient and provide for improved safety and handling.

Figure 1.1: Typical Twin Axle Caravan (Jayco, 2016)

1.3   Research Aims and Objectives

The original intent of the research was to utilise a caravan prototype developed by Toowoomba based caravan manufacturer Airflow Caravans which was designed with improved features which were intended to improve the fuel efficiency of the tow vehicle. Unfortunately due to certain circumstances Airflow Caravans were not able to continue providing in-kind support for this research. This required an additional task to identify a suitable caravan and tow vehicle alternative for use in this study.

The project specification as detailed in Appendix A was therefore produced to outline the deliverables of the research as an extension of the research conducted by Briskey (2013), titled 'Improving Caravan Design by Modelling of Airflow'. The project is broken down into seven phases, with three additional phases to be conducted if time permits. The objectives of the study are as follows:

1.   Research the background information related to caravan drag profiles and towing vehicle performance through CFD modeling.

2.   Research geometry and performance data for subject caravan and tow vehicle.

3.   Create a 3D model of the Caravan and Tow Vehicle for use in CFD analysis.

4.   Validate 3D model using a headwind analysis.

5.   Undertake CFD simulation of current prototype under cross wind conditions.

6.   Investigate and propose performance enhancing modifications to the initial baseline design.

7.   Perform a CFD analysis and parametric study on the modified caravan.

If time permits the following tasks have been proposed in order to expand on the main research conducted. They are as follows;

8.   Propose further modifications.

9.   Investigate the dynamic stability of the caravan and tow vehicle when subjected to cross wind air flow.

10.   Perform transient simulation of caravan/tow vehicle movement due to crosswind loading.

1.4   Dissertation Outline

The following provides a general overview of each chapter of this dissertation.

1.4.1 Chapter 1 – Introduction

The structure of the dissertation is presented along with an introduction to the research project. Background information relating to the selection of the problem, an outline of the study and the research objectives are also documented. A summary of the project methodology is provided along with consequential effects and risks associated with undertaking this research.

1.4.2 Chapter 2 – Literature Review

This chapter presents a comprehensive literature review undertaken to understand the scope of the research. Areas of literature reviewed and documented include; aerodynamics,

crosswind airflow effects on transportation vehicles and their optimization. Computational Fluid Dynamics techniques and applicability to this study is also presented. This literature review expands on the literature review conducted by Briskey (2013) in which the influence of cross wind flow becomes the priority of this study.

1.4.3 Chapter 3 – Research Methodology

This chapter covers the methodology which is used to analyze the effect a crosswind will have on the caravan/tow vehicle combination in terms of generating drag and other aerodynamic forces. The process of generating a model to represent the vehicle geometry, application of required meshing and the subsequent grid independence study is detailed in addition to the setup parameters for the CFD analysis and pre-optimization solutions.

1.4.4 Chapter 4 – Pre-Optimization Study

This chapter presents the results of the baseline caravan/tow vehicle combination configuration CFD study. Visual representations of airflow are presented and discussed in detail. Recommendations are made to explore modifications that will be subsequently evaluated in a post optimization parametric study.

1.4.5 Chapter 5 – Parametric Study on Baseline Configuration

This chapter details the optimization of the baseline model and details the method to conduct a parametric study to produce new results that reflect the impact that the proposed modifications have had in comparison to results detailed for the baseline configuration in Chapter 4.

1.4.6 Chapter 6 – Results & Discussions

This chapter presents the results of the post optimization parametric study. It presents data to present a comparison between pre and post modification results and provide both a quantitative and qualitative assessment of the effectiveness of each featured modification.

This chapter also details further work and details issues encountered during the study and potential for re-evaluation. Areas of research currently out of scope are detailed with any improvement suggestions made to how the study can be conducted in future.

1.4.7 Chapter 7 – Conclusion

This chapter provides a summary of the outcome of the study and evaluates its success against the project specification and original objectives. A final recommendation is presented on a configuration that provides the greatest improvement in aerodynamic efficiency and road handling. This chapter also details further work and details issues encountered during the study and potential for re-evaluation. Areas of research currently out of scope are detailed with any improvement suggestions made to how the study can be conducted in future.

1.5   Consequential Effects

In order to provide an accurate assessment regarding the impact that this project will have on the wider society currently involved in using caravans, it is important to understand some of the important factors that affect customers experiences and expectations about the topic.

These factors can be grouped into two main categories; sustainability and safety.

As a professional engineer, one is expected to make a conscientious effort to address these two concerns amongst others in the pursuit of engineering excellence. Engineers Australia (EA) has promoted its Code of Ethics in order to ensure that its members exercise their responsibilities as professional engineers with due diligence and professionalism.

1.5.1 Ethical Considerations

Tenet 4 of the Code of Ethics relates to an Engineer's responsibility to promote sustainability (Engineers Australia, 2010).

The task involves research into the effects that drag has on a caravan/tow vehicle combination and is focused on identifying the drag produced by crosswind flow, and how this leads to higher operating costs through the increase in fuel consumption figures for the tow vehicle. The effects of increased fossil fuel consumption are readily seen in the environment through pollution and it is therefore seen as a major concern for engineers

that are concerned with offering consumers an option that is both financially viable for them whilst also ensuring that any ill effects on the natural environment are minimized.

In addition, the safety of all persons utilizing the technology is to be a priority and a conscientious effort is to be made to ensure that the engineering rigor applied to all phases of the development is adequate to meet this objective.

1.5.2 Risk Assessment

The risks associated with both the conduct of this study and the research deliverables can be separated into two distinct categories.

1. Risk associated with adopting recommendations and utilization of research data from this dissertation as the basis of other research.

2. Risks and Hazards associated with the completing the research project in line with WH&S principles

In addressing the first point, it is important to note that the research is to be conducted utilizing available information captured at the time when the literature review was conducted. Prior to implementing any recommendations an additional validation study is to be conducted utilising scale model representations, tested in wind tunnels and where possible extensive road testing to ensure that any anomalies in CFD findings are identified and any areas of research outside of the scope of this task are addressed where required.

A risk assessment has been conducted and documented in Appendix C - Risk Assessment for the risks associated with point 2 of this section.

1.6 Summary of Methodology

Detailing the methodology used in performing this study is a fundamental requirement in order to give the research direction and to provide a roadmap to highlight the methods used to obtain the deliverables as per the Project Specification.

Following the literature review phase, the project requires the creation of the models required for the CFD simulation. The creation of the models can be performed utilizing ANSYS Workbench or alternatively imported from a 3D modeling package such as Creo Parametric or Autodesk Inventor Professional. Due to familiarity with the CREO modeling

package it has been selected as the software that will be used to model both the caravan and tow vehicle geometry.

The models are then required to be examined against existing data to ensure that a comparable result between published data, dimensioning and physical features exists. This process will ensure that a relatively high level of confidence is achieved by using models that accurately represent the actual product. This is achieved by ensuring that the approximation of features used in the model do not significantly alter the aerodynamic profile of the vehicle. In addition the mesh used is to be refined until the simulation results don't change significantly ensuring that numerical errors are as small as possible. For the purpose of this study it has been decided that a value of no greater than 1 percent error is acceptable in order to proceed with the CFD study. The caravan and tow vehicle models are then combined to form the combination that will be evaluated in a headwind airflow configuration. This process allows for the validation of the CFD pre-processing and solver function to ensure that a suitable setup is identified and documented. Following the establishment of a suitable test procedure, the baseline caravan and tow vehicle combination can be modeled under crosswind airflow for the remainder of the study. To allow for a good coverage of crosswind airflow effects on the vehicles, the direction of the flow impinging on the vehicle will be taken at 15, 30, 45 and 60 degrees from the front of the stationary vehicle. The results obtained from the simulation will be analyzed and areas of the caravan's geometry and towing configuration identified for modification. Based on some of the aerodynamic modification features identified through the literature review, modifications will be identified and implemented on the model for the purposes of conducting a parametric study.

The modified geometry will then be simulated under the same test conditions as used in the baseline study and an assessment of any efficiency gains undertaken. These efficiency gains will be translated from reductions in drag to an improvement in fuel efficiency of the tow vehicle.

The findings will then be documented in the form of a dissertation and recommendations will be presented, allowing for any viable solutions to be explored further in future research where required.

1.7 Resources Requirements

The following resources have been identified as required in order to complete this research.

- ANSYS 16.2
- Access to license through USQ server
- 3D Modelling Software (CREO Parametric, Inventor Professional etc.)
- ANSYS Tutorials and Learning Documentation
- Time allocated to conducting the research

1.8 Project Timelines

Appendix B - Project Timelines documents the project timelines and schedule. It aims to provide some guidance in stipulating key milestones and ensuring that there is accountability to ensure deadlines are met on time. The project timeline is represented graphically by way of a Gantt chart.

CHAPTER 2 – LITERATURE REVIEW

2.1 Introduction

In order to understand and get an appreciation of current design practices and operating considerations for caravans, it is necessary to undertake a critical review of existing literature. This literature review will focus on the research conducted into the effects of crosswind aerodynamic loading on various types of transportation vehicles, including cars, trucks and trains. A review of this literature will aim to demonstrate how current research in this area has led to the evolution of design practices in the caravan industry, through extending the design optimisation and analysis principles towards caravan design through the implementation of Computational Fluid Dynamics (CFD) techniques.

2.2 Study of Aerodynamics

Throughout history the concept of 'aerodynamics' has been an area of science that has seen a significant effort applied to understanding the science behind the movement of air and its influence on external bodies.

The widely accepted definition for the term 'aerodynamics' is defined as the study of air in motion. It concerns itself with the motion of air and other gaseous fluids and deals with the forces exerted on a body as it moves through the fluid as proposed by (Johnston, 2016).

Crosswind aerodynamics deals with airflow that does not move in the plane of vehicle travel, but moves at an angle relative to the direction of travel. The crosswind can be depicted as having a two velocity vectors to define its forward and perpendicular velocities with a resultant velocity to define the angle which defines the direction of the wind source. The Cambridge Dictionary, (2016) defines a crosswind as a wind blowing at an angle to the direction a vehicle is travelling.
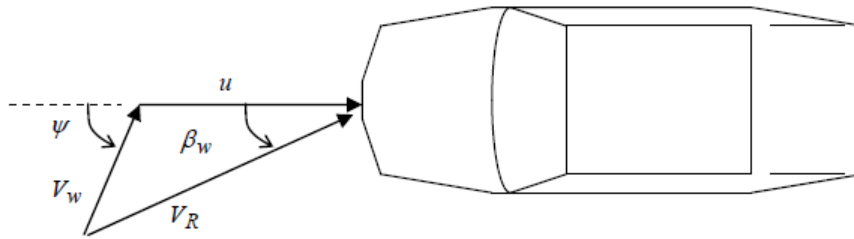
Figure 2.1: Crosswind Velocity Components (Mansor et al. 2013)

2.3 Crosswind Aerodynamic Effects in Transportation Vehicles

The flow of air around the body of a moving vehicle due to crosswind flow leads to the introduction of pressure loads that play a major role in both the generation of aerodynamic drag and the stability of the vehicle predominantly in the roll and yaw axis. The literature reviewed can be broken down into two main areas, these are;

• Literature concerned with Aerodynamic Drag forces and coefficients, and

• Literature concerned with the dynamic response of vehicles to crosswinds

The purpose of this literature review will be primarily to understand how the aerodynamic forces in play contribute to the generation of drag on the vehicle and how this drag leads to increases in fuel/energy consumption. The land based vehicles focused on in the review include cars, trains and truck-trailer combinations.

2.3.1 Cars

Early forms of the car displayed very little ingenuity when it can to shape and form. At the turn of the century in 1902 manufacturers across both Europe and America that had pioneered transportation advancements focused on horse drawn technology had begun to turn their attention to self-propelled transportation which harnessed the power of both the steam and internal combustion engine. The Model T Ford designed in 1908 and later mass produced in 1913 by Henry Ford had a top speed of about 70 km/h with any additional increase in speed obtained by upgrading the engine (Dorling Kindersley, 2016).

Figure 2.2: Model T Ford (Dorling Kindersley, 2016)

The 1940s saw huge advances in the development of highways to facilitate the movement of a larger amount of vehicles in order to transit between major city hubs with ease. (Kee et al (2014), attributes the improvements made to automobiles to the expansion of narrow and somewhat poorly sealed roads which were gradually being replaced with multiple lane road sections, which enabled the movement of transport vehicles at much higher speeds than previously experienced.

The greatest advancement in car design came with the pursuit for speed which was coveted by the racing industry. The concept of measuring drag as a coefficient allowed designers to focus their attention on getting the shape of their car designs to resemble a 'teardrop' or 'bullet' shape, which were both known through experimentation to offer the lowest Coefficient of Drag (Cd) values.
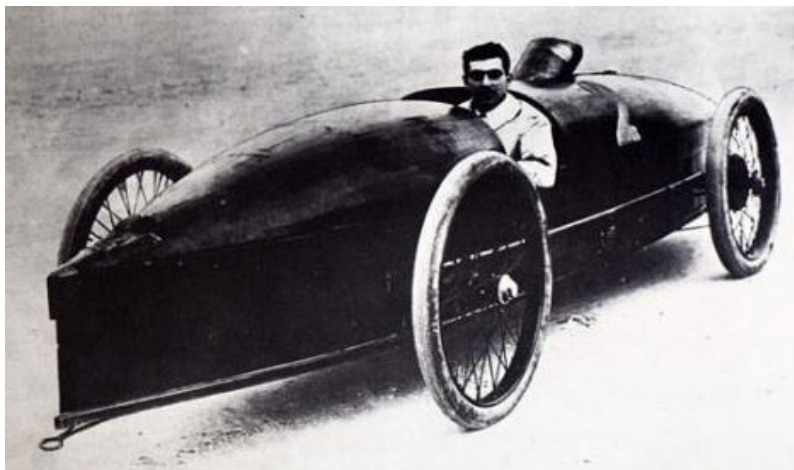
Figure 2.3: La Jamais Contente (The Truth about Cars, 2016)

The car is generally considered to be a bluff body with coefficients of drag generally seen within the range of 0.3 to 0.4.

2.3.2 Rail Transportation

Another mode of transportation which has seen vast changes since inception is rail travel. The evolution of the rail industry has historically shown the greatest increase in land speed reached over a period spaning approximately 180 years (UIC, 2015). The year 1830 saw the steam powered locomotive named 'Rocket' reach a speed of 50 km/h. Advancements in technology regarding the power system and the transition into the electric age saw rapid increases in speed up to 210 km/h in 1903 and further refinements in shape and power transmission in the 1980's saw the development of what is today labelled 'High Speed Rail' with current speed record of 574 km/hr set in France by the AGV Italo in 2007.

With the pursuit of speed in mind, designers opted for more streamlined shape profiles and experimented with lighter weight materials coupled with higher performance engines or power transmission systems. This in turn increased the sensitivity of the vehicles to the external forces of the airflow. Of great concern, the impact of crosswind airflow and its ability to produce significant side loading problems to the carriages travelling through clearings in high wind areas had led to numerous accidents worldwide. Asress, (2014) makes particular mention of the work that many European transport regulatory bodies have undertaken in an attempt to minimise the prevalence of wind related train accidents by establishing design and operating legislation. It is important to note that the problem can only be properly addressed when both the vehicle design and the infrastructure that it operates within are given equal attention. Figure 2.4 depicts serious accidents that occurred in Austria in 2002 & Switzerland in 2007 which was directly attributed to crosswind loading on the trains which caused it to de-rail at speed. The trains were subject to crosswinds in the vicinity of 30 m/s.

Figure 2.4: Crosswind related Train Accidents (Asress & Svorcan, 2014)

Of major importance, as trains have evolved in design over the past century the materials that are used in their manufacture have also evolved significantly. The use of lightweight materials has contributed significantly to the reduced mass of these high speed vehicles and subsequently have increased their sensitivity to crosswinds. The transition towards streamline and at times elongated 'bullet' style noses have led to the generation of significant negative pressures on the leeward side of the train, which contributes significantly to the stability of the train when travelling at high speed in cross wind environments.

The aerodynamic characteristics of vehicles subjected to a crosswind is somewhat complicated to assess due to the influence of external structures or barriers between the airflow source and the surface of the vehicle. Suzuki, Tanemoto & Maeda (2003) identified various contributing factors when assessing the effect crosswinds have on train derailments. Factors such as narrow gauge rail tracks can facilitate the process of derailment once the crosswind has disturbed the lateral stability of the train carriage, particularly during transient loads. Figure 2.6 depicts the unstabling effect that a transient air load (wind gust) has on the trailer of a truck travelling at high speed.

For this particular study the airflow will be dealt with as 'steady state' and the environment in which the caravan is travelling through is straight and level with no obstacles to affect the profile of the airflow reaching the caravan structure. This removes the additional complexities introduced by transient airflow and more complex turbulent models.
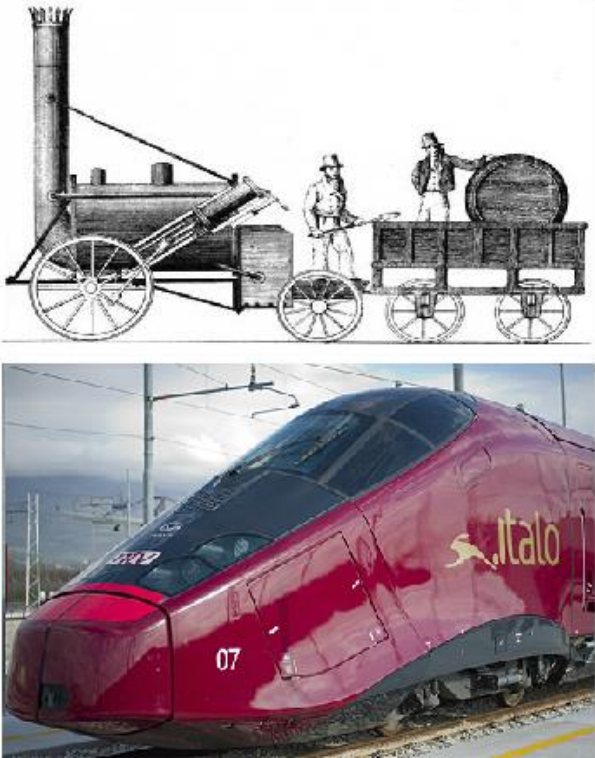
Figure 2.5: 1830's 'Rocket' Steam Locomotive & AGV Italo Bullet Train

Figure 2.6: Truck Rollover Incident due to Crosswind (WILX News, 2014)

2.3.3 Truck & Trailer

The trucking industry according to National Transport Insurance (2011) was worth over $35 billion to the Australian economy with projected revenue increasing to over $45 billion by 2016. Statistically the 'work horse' of the truck industry is the articulated truck which carries over 75 percent of all freight moved across Australia although only accounting for 2.3% of all registered trucks.

With the increase in global fuel prices, freight operators have been put under considerable pressure to find ways to minimise direct operating costs maximising their company profit margins. To do this many operators have turned to investing in aerodynamically efficient vehicles and others have undertaken modifications to existing fleets in order to reduce drag and improve fuel economy.

According to (Aeroserve Technologies Ltd, 2006) researchers looking into truck drag minimisation have concluded that the following four areas concerning trucks that are responsible for the generation of aerodynamic drag. They are;

1.   Front of Tractor
2.   Tractor-Trailer gap
3.   Wheels and Wheel Arches

4. Rear of Trailer

Of particular importance to designers is the concept of separated flow. As the airflow that makes its way around the body of the truck flows over a sharp corner or bend in the structure it separates from the surface and transitions into turbulent flow. Aeroserve Technologies Ltd (2006) research suggest that with only headwind flow considered the airflow that separates itself from the tractor is generally expected to reattach itself to the trailer approximately one-third of the distance down the length of the trailer. When crosswind flow is considered the airflow very rarely reattaches itself to the leeward side of the truck. Corner radiuses of less than 6 inches on trailer bodies is also considered to promote the separation of airflow from the body.

Drag minimisation strategies for trucks are intended to address the problem pressure drag effects on power required and subsequently aim to reduce fuel consumption. Patten et al. (2012) indicate that friction drag on the surface of a vehicles body only accounts for 10% of all drag forces. It is therefore not considered feasible to allocate significant time, effort and resources to addressing this issue. The main focus of drag minimisation involves the reduction of pressure drag.

Table 1:Truck Power Consumption Figures (Patten et al. 2012)

Vehicle Speed	Aerodynamic	Rolling & Accessories
32 km/h (20 mph)	28%	72%
53 km/h (33 mph)	33%	66%
64 km (40 mph)	36%	64%
80 km/h (50 mph)	50%	50%
96 km/h (60 mph)	62%	38%
105 km/h (65 mph)	67%	33%
113 km/h (70 mph)	70%	30%

Table 1 depicts the power required to overcome both Aerodynamic Forces and Rolling Friction/Accessory power draw. Initially at the lower vehicle speeds the majority of the power required is used to overcome the rolling resistance and power the accessories. As the velocity of the vehicle increases the drag forces due to air resistance start becoming more prominent as can be seen when travelling at highway speeds where air drag accounts for over 65% of all power required.

2.4   Selection of Tow Vehicle for Study

The most popular tow vehicles as published by Caravan World, a popular website for caravan owners lists the following vehicles in order of popularity;

1.   Toyota Landcruiser 200 TDV8
2.   Range Rover SDV6 3.0
3.   Land Rover Discovery 4 3.0
4.   Jeep Grand Cherokee 3.0
5.   Lexus LX570

The study conducted by Briskey (2013) utilised the Land Rover Discovery 4 as the tow vehicle. This study will continue to utilise the current release of this vehicle as there is currently established baseline data that will be used for comparison purposes. In addition, when comparing the shape profile of the top 5 vehicles, the Discovery 4 provides a reasonably similar profile to the other vehicles in the top four positions of this list.

Figure 2.7: Land Rover Discovery 4 (Without-a-Hitch, 2016)

2.4.1 Tow Vehicle Characteristics

When determining the aerodynamic efficiency of a vehicle design the term Coefficient of Drag (C_d) is used to describe how easily the vehicle can move through the air.

The coefficient of drag is defined by most literature sources as;

$$C_d = \frac{2 \times F}{\rho \times v^2 \times A}$$

where;

F = Drag Force (N)

ρ = Density of the air (kg/m^3)

v = Fluid Velocity (m/s)

A = Cross Sectional Area (m^2)

As aerodynamic drag increases with the square of the velocity, the drag increases exponentially with speed requiring more power to be applied to overcome the drag force in order to maintain its speed.

The coefficient of drag value provides a quick method to compare vehicles in order to assess how aerodynamically efficient they are in relation to each other. A streamline vehicle design such as the Mazda 3 features a Cd of 0.26 whilst the less streamlined Land Rover Discovery 4 features a Cd of 0.4 (Carfolio,2013).

A specification sheet has been included in Appendix D listing the dimensional characteristics of the 2016 Land Rover Discovery 4.

2.5 Caravan Development

2.5.1 Caravan Classification

There are a large variety of caravan models available to the consumer and are marketed towards the users requirements. They can be described under the following categories;

- Conventional Single Axle
- Twin Axle
- Pop Top Caravans
- GRP Fibreglass
- Camper Trailer
- Fifth Wheelers

Conventional Single Axle caravans are generally the most common type of caravan in use. They can accommodate two to six people, with all the normal amenities. These caravans usually range in size between 3 to 6 metres in length.

Figure 2.8: Conventional Single Axle Caravan (Swift Group , 2016)

Twin Axle caravans have become more common over the past decade as manufacturers build larger and heavier caravans in order to carry more equipment on board. The advantages of having twin axle included added stability and better towing on the road. They do however require more skill to manoeuvre in tight areas.

Figure 2.9: Twin Axle Caravan (Jayco, 2016)

The Pop-Top caravan consists of a standard caravan body with an extendable canopy that raises in order to provide more headroom. The advantage of such design is the ability to reduce the frontal area of the caravan whilst being towed. This results in the reduction of drag, improving fuel consumption for the tow vehicle.

Figure 2.10: Pop Top Caravan (Jayco, 2016)

GRP Caravans, predominantly manufactured from fibreglass are commonly the smallest, most compact type of caravan. They are fairly lightweight and although featuring very little in the way of amenities, feature mobility in sleeping facilities at reasonable cost.

Figure 2.11: GRP Caravan (Jayco, 2016)

Camper trailers offer the ultimate in flexibility and affordability. They feature a low design which is easy to tow. Once in position these caravans can open up and expand into various configurations. These trailers are very easy to store and can be towed with a regular sedan.

Figure 2.12: Camper Trailer (Jayco, 2016)

Fifth Wheelers are larger variants of the single and twin axle caravans. They do not feature a standard hitch but utilise a special hitch that can only be used with utility vehicles that have an articulated towing connection point fitted to the tray. They are by far the largest type of caravan and have the ability to expand into much larger living spaces once in position.

Figure 2.13: Fifth Wheeler (Grey Wolf, 2016)

2.6 Computational Fluid Dynamics

Computational Fluid Dynamics (CFD) is a branch of fluid mechanics in which the Partial Differential Equations (PDE) used to define fluid flow are approximated by algebraic equations which are able to be solved using computer resources. Kuzmin (2012) describes the versatility of CFD in able to solve a variety of complex problems ranging from; meteorological phenomena, heat transfer, combustion, complex flows to human body functions such as breathing. Its versatility is what makes it such a valuable tool to conduct studies that previously would have taken a very long time to complete.

2.7 Application of CFD to Vehicle Aerodynamics Analysis

Computational Fluid Dynamics use over the past 30 years has increased significantly allowing for greater flexibility and cost minimisation in many engineering projects involving the design of both land and air vehicles. Johnson et al. (2003) has provided insight into the evolution of design practices at the Boeing Company over three decades. Design methods which mainly consisted of; analytic approximations, wind tunnel and flight testing, made way to Navier Stokes equation approximations performed by powerful computers with relative ease.

The role of wind tunnels to provide data regarding lift and drag has been an effective method of validating design features using scale models. Johnson et al. (2003) mentions that certain errors and complexities are introduced in the wind tunnel due to the requirement to mount the model within the evaluation domain. This mounting method can

introduce interference issues with the airflow. Figure 2.14 depicts a typical wind tunnel set up for both a land based vehicle (a) and an air vehicle (b).

(a) (b)
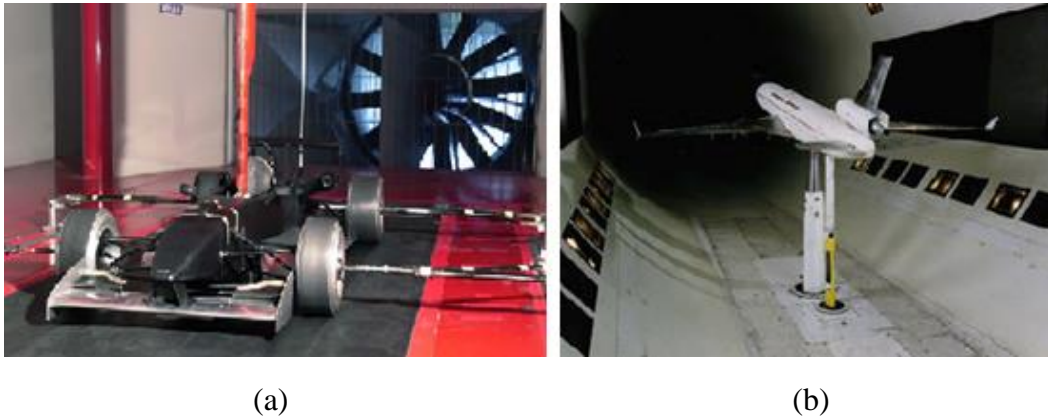
Figure 2.14: Wind Tunnel Test Setup (Autoevolution & NASA)

Wind tunnel testing offers the ability for designers to utilise 'real' conditions to test their designs over a vast range of atmospheric parameters. Johnson et al. (2003) attributes the success of CFD to its ability to provide an inexpensive solution to preliminary testing and optimisation through the extrapolation of known data with the aim of providing a baseline for future experimentation of operating parameters. It is important to note that the use of CFD on its own is not an ideal design validation technique with most industries where CFD techniques are commonly employed utilising a combination of CFD and physical testing to gather the required data necessary to evaluate designs.

2.8 Application of CFD to Caravan Analysis

The majority of literature consulted regarding caravan CFD analysis is centred around simulating the frontal drag forces. Caravan manufacturers in general have not expended additional resources and efforts to revisit their designs which have been put into production. Universities in collaboration with engineering companies which focus on CFD analysis have collaborated recently to undertake studies with the aim of reducing aerodynamic drag on existing popular designs. Glynwr University, (2011) performed a study in collaboration with ASTUTE on a popular caravan design manufacturer by The Fifth Wheel Company Ltd. The feasibility study aimed to study the aerodynamic flow of air around the caravan structure and make a comparison between the effects different towing vehicles had on the generation of drag. As a rule of thumb, aerodynamic drag forces acting on commercial vehicles can contribute up to 60% of fuel consumption figures.

The study aimed to reduce aerodynamic drag by up to 20%. Through the use of CFD, modifications were proposed and recommendations made which led to a potential decrease in drag figures of up to 34% from the original design. This resulted in a decrease of 22.5% of the power required to tow the caravan at speed, whilst reducing the size of the trailing wake. Figure 2.15 depicts an example of the results obtained during this study.
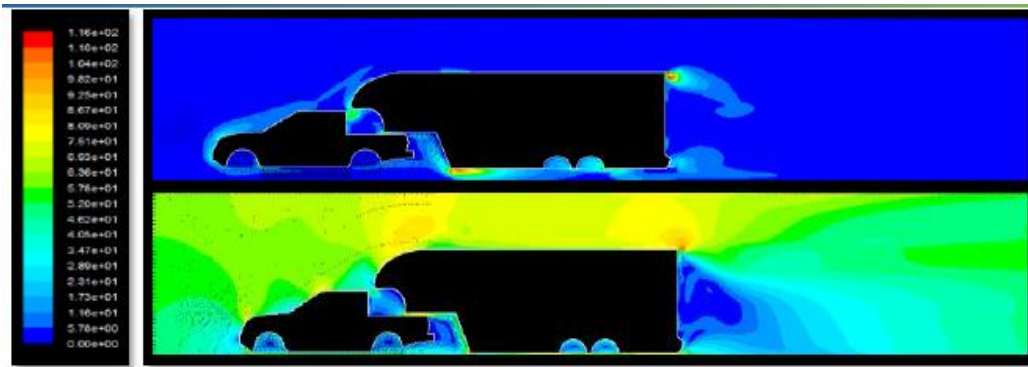
Figure 2.15: CFD Simulation-Flow Modelling (Glyndwr University, 2011)

Another significant study was conducted by the Swift Group, a caravan designer based in the United Kingdom. The study was brought about by the need to find efficiency gains that were intended to offset the rising cost of fuel. (Swift Group, 2011) proposed that manufacturers claimed through marketing that their caravans were aerodynamic but this was mainly based on subjective data using rudimentary methods such as towing trials.

Swift Group contracted a CFD specialist to undertake a 3D scan of their caravans and utilise these models to simulate the flow of air around the caravan. This CFD study was complemented by concurrently running wind tunnel tests on their caravans. As a result Swift Group was able to implement a weight reduction program and coupled with further streamlining of their caravan designs were able to significantly reduce the running cost involved with towing their products. Figure 2.16 depicts a near wall velocity study conducted using CFD.
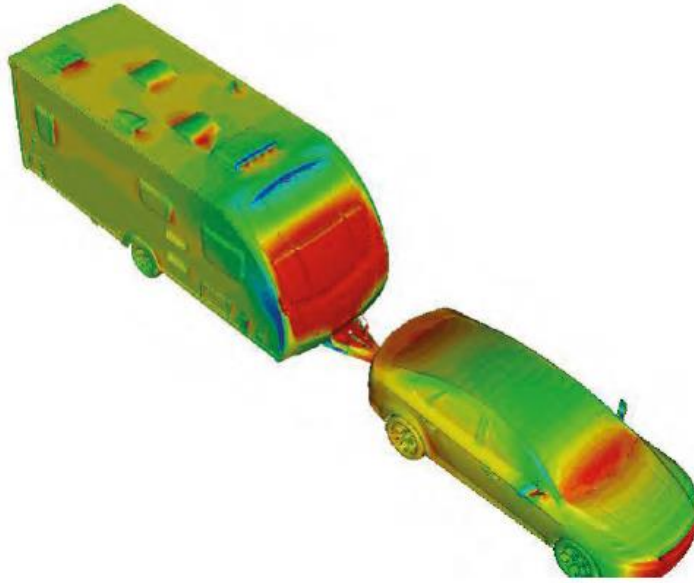
Figure 2.16: Near Wall Velocity CFD Study (Swift Group, 2013)

Although there is significant evidence available to confirm the benefit of conducting a CFD study on caravan from a frontal profile perspective, the effect of cross wind influence on the geometry is not as widely published as is found with other transportation methods such as trucks and trains.

2.9   CFD Pre-Processing

An essential function of performing a CFD analysis involves the preparation of the model geometry and the mesh in order to configure the solver to be able to produce the best results possible with as little effort as possible. At a minimum the process can be defined by (ANSYS Release 14.5 Documentation, 2012) as;

1. Create the geometry
2. Simplify the geometry
3. Define the mesh resolution required
4. Define the mesh type required
5. Assess computing resources available

2.9.1 Development of Geometry

An important consideration when configuring the CFD software package to commence solving a problem is to ensure the geometry in which the airflow will be simulated through is optimised for the particular model being tested. (Keating, 2010) states that by following some pre-processing guidelines, reliable results can be obtained time after time. In order to set up the simulation environment optimally the following questions should be asked;

- What do you want to do and gain from the CFD analysis?

- What are the driving parameters?

- What zones need to be separate for constraints or post processing?

- What fluids zones will be replaced?

- What level of geometric representation is needed?

It is also emphasised that small changes can have large effects.

2.9.2 Mesh Generation

Mesh quality is an important consideration when undertaking a CFD analysis. Keating, (2010) agrees with other literature sources in emphasising that the quality of the mesh goes a long way to providing accurate and reliable results. Generating a mesh often requires significant time and computing resources depending on the complexity and geometric configuration of the mesh required. It is however important to note that at this point the investment made in generating a good mesh pays greater dividends when it comes to generating a solution.

Bakker, (2002) states that hexahedral meshes offer the best solution, with the accuracy of the solution becoming even greater when the mesh grid lines are aligned with the flow. Quality of a mesh is defined by the following three features; Skewness, Smoothness and Aspect Ratio.

Skewness in the cell geometry should be avoided. Increases in cell size should be incrementally smooth and finally an aspect ratio for mesh cells of 1 should be strived for

as featured in squares and equilateral triangles. Keeping the mesh quality high will ensure that solutions are as accurate as possible.

2.9.3 Establishment of Boundary Conditions & Turbulence Models

In order to establish the context of the simulation and define the domain in which the solver will calculate for, it is vital that the correct boundary conditions be established and that the correct model be selected depending on the type of problem. There is significant amounts of literature which highlight the pros and cons of the most common turbulent flow models employed by the major CFD software packages. These models aim to represent the Navier-Stokes equations as accurately as possible through the setup of a simulated wind tunnel, however accuracy is limited by the amount of processing resources and the discretisation size of the domain.

Frei (2013) conducted a comparison exercise to highlight the advantages and disadvantages of the most commonly used turbulent models used in CFD practices. Table 2 presents the findings of this review.

Table 2: Turbulence Model Comparison (Frei, 2013)

Model	Advantages	Disadvantages	Applicability
k-epsilon (k-ε)	Good Convergence Rate Requires less computing resources Reasonable prediction of different flow types Utilises wall functions	Applicable only to fully turbulent flows Difficulty in predicting the following; Swirling or rotating flow Adverse pressure gradients	Airflow simulation around bluff bodies Industrial applications Simulation of Complex geometries Axisymmetric jet flow
k-omega (k-ω)	Ability to simulate for flows that feature; Internal Flows Separated flows Jet airflow	Sensitive to initial guess of solution. Difficulties in reaching convergence Requires pre-processing through k-epsilon model to aid in accuracy	Simulation of Internal flows. Used in modelling fluid flow through pipes and ducts.
Low Reynolds k-epsilon	Higher Accuracy in modelling lift and drag forces.	Requires higher computing resources	Simulation of Lift and Drag forces around bodies. Heat flux simulation problems
Shear Stress Transport (SST)	Accurate for solving flow near walls. Utilises k-epsilon modelling technique for free stream flow and k-omega model in the wall region.	Somewhat slow to reach convergence.	Effective in handling similar problems as detailed in k-epsilon and k-omega sections.

The two equation models (k-ε & k-ω) feature the greatest flexibility for most applications. Frei, (2013) promotes the k-epsilon model as the most versatile of the turbulent models as it combines the two variables k; turbulent kinetic energy, with ε ; the rate of kinetic energy dissipation, in order to provide somewhat quick results with known inaccuracies in dealing with laminar flow. The true effectiveness of the turbulent models are centred around the ability of the model to capture what is occurring in the boundary layer between the laminar layer at the wall of the surface and the turbulent layer above. Figure 2.17 depicts the boundary profile of the airflow. By utilising wall functions in models such as k-epsilon in order to simulate flow in the buffer region, the model can utilise approximations in order

to reduce the computational requirements and therefore leading to a more rapid and less resource intensive solution. On the other hand, for increased accuracy at the boundary layer the k-omega model provides a greater degree of accuracy, due to its computational method without the use of wall functions. It is however noted from Table 2 that the resources required are much higher and convergence is also somewhat difficult to achieve.

The Shear Stress Transport (SST) method provides a more accurate solution when considering the boundary layer. Karthik (2011) defines the SST model as an eddy-viscosity model which combines the previously discussed two-equation models in combination to model the buffer layer with greater accuracy. The k-ε provides a model for the region outside the boundary layer, whilst the k-ω models the region inside the boundary layer.

When assessing the requirement to use a particular model for a study, two main considerations need to be factored into account. Frei (2013) highlights the requirement to utilise a problem mesh which is as simple as it can be in order to obtain the desired level of accuracy. Secondly, the turbulence model selected should provide results which strike a balance between computational resources, processing time available and accuracy of the solution.
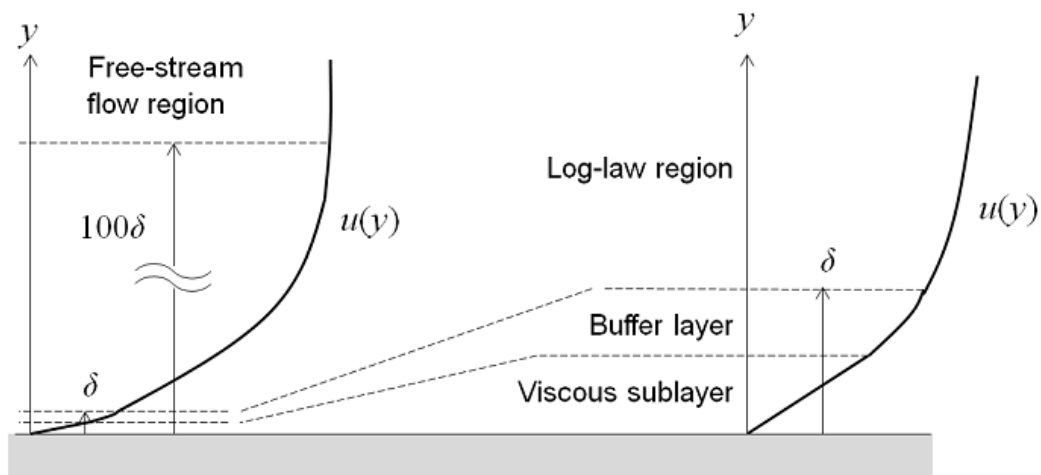
Figure 2.17: Flow regimes at the Wall Interface (Frei, 2013)

2.10 CFD Solver

The simulation process performed by CFD software packages such as ANSYS generally utilise a two-step approach in order to compute a solution (ANSYS Fluent Documentation, 2006). These steps can be defined as Numerical Model Setup and Computation/Monitoring of solution. Together they form the core function referred to as the Solver Execution.

The numerical model setup process generally comprises the following elements according to Ahmadi & Nazridoust (n.d);

1. Selection of an appropriate physical model for the simulation: combustion, turbulence etc.
2. Define the material properties; fluid, solid or mixture.
3. Prescribe operating conditions; temperature, pressure, velocity etc.
4. Prescribe the boundary conditions
5. Produce Initial Solution
6. Set up Solver Controls
7. Monitor Convergence

The computation and monitoring phase deals primarily with the discretization of the conservation equations or Navier Stokes equations which are solved iteratively until convergence is reached. Convergence is deemed to be obtained when the difference in solution data from one iteration to another is negligible verifying the numerical accuracy of the solution. Convergence can therefore be used to validate the accuracy of a solution as it changes over time.

Convergence is monitored through the use of 'residuals'. Kuron (2015) describes residuals as one of the most fundamental measures of iterative convergence, as it provides a direct numerical representation of the error involved in the solution of the system of equations. Figure 2.18 depicts an example of a common residual plot with the variable value (Y-Axis) plotted against an Accumulated Time Step (X-Axis).
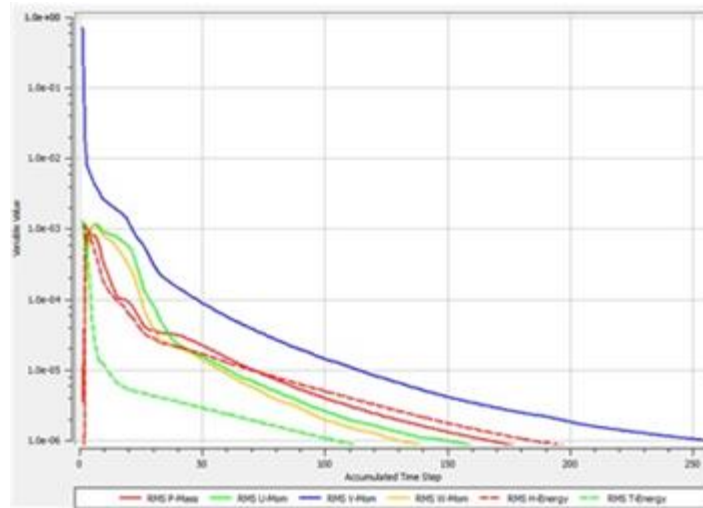
Figure 2.18: Residual Monitors

It is important to note that because a residual represents the absolute error between two iterations of a solution it is therefore ideal that the error be reduced to a value as close to zero as possible. Throughout the majority of literature reviewed convergence can be deemed to be roughly achieved when the Root Mean Squared (RMS) residual levels are less than a value of 1×10^{-4} and residual levels of 1×10^{-5} are deemed to be well converged (Kuron, 2015).

Convergence with regard to CFD applications can also be identified through the monitoring of points of interest. Gelman et al (2003) describes the error in defining convergence if a simulation is not left to run for an extended period of time. By monitoring individual points in a variable solution over a defined number of iterations, convergence is said to be reached when fluctuations decrease to a small amount in the order of 1×10^{-4} - 1×10^{-6}. This can usually be represented by a relatively flat 'tail' in the plot as depicted in Figure 2.19.
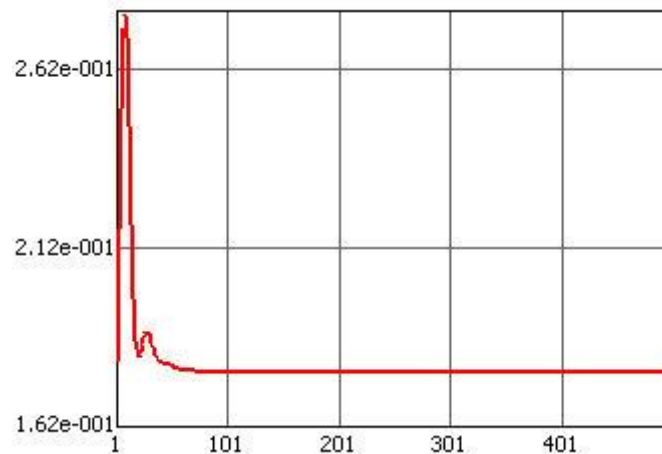
Figure 2.19: Monitor of Point of Interest (Thoms, 2007)

2.11 CFD Post Processing

Once the solver has performed the simulation and has generated the required data sets, the data must be processed through specific software, namely ANSYS CFD Post, which provides a post processing capability to ANSYS Fluent and CFX. This process is required in order to manipulate the data and generate the required numerical and visual representations that can be tailored to the output parameters required. These representations can take the form of streamline plots, pressure gradients and velocity scalars/vectors as well as reports which can depict histograms of data. An important consideration in performing effective post processing functions is to gain a good understanding of what data is required in order to draw the necessary conclusions and how that data can be manipulated to produce effective graphical representations of information to support both quantitative and qualitative discussions of results.

2.12 Force Coefficient Calculation

Malviya, Gundala & Mishra (2009) undertook a study to determine an effective way to calculate the coefficient of drag, lift and side force for ground based vehicles subject to a crosswind.

The three main equations used in the calculation of these forces are;

$$F_D = \frac{\rho C_D A v^2}{2}$$

$$F_L = \frac{\rho C_L A v^2}{2}$$

$$F_S = \frac{\rho C_S A v^2}{2}$$

Where C_D, C_L and C_S represent the coefficients of Drag, Lift and Side Force respectively.

A represents the characteristic frontal area of the vehicle and can be calculated for different areas presented to the flow when the vehicle is under yaw. The trigonometric relationship for the characteristic area A is calculated using the equation;

$$A = (l \times sin\alpha + w \times cos\alpha)h$$

Where l = length of vehicle,

w = width of vehicle, and

h = height of vehicle

In order to calculate the characteristic area of the vehicle combination it is common practice to represent the vehicle as rectangular boxes multiplying the area by a factor of 0.85 for cars and a factor of 1 for truck/trailer combinations. It was decided that for this scenario that a value of 0.95 would be appropriate given the rectangular nature of the vehicles in question.

2.13 Literature Review Summary

It is evident throughout the literature reviewed that designers, manufacturers and researchers have conscientiously applied themselves to the purpose of enhancing the aerodynamic efficiency of vehicles in order to reduce operating costs and benefit from increases in speed and handling.

From the literature review it is also evident that there has not been any specific attempt to address the effect that crosswind flow has on a car and caravan combination. It is however noted that the studies conducted into truck & trailer combinations and high speed trains under crosswind raise some interesting points, these observations and suggestions for modifications can be carried across to the caravan.

The literature concerning the use of Computational Fluid Dynamics by computer simulation programs such as ANSYS has been reviewed with valuable insight gained into how the approach can be useful in order to simulate how a system will perform in 'real world' conditions. The literature provided valuable guidance in how to set up the problem, run the simulation and then interpret the results.

CHAPTER 3 – RESEARCH METHODOLOGY

3.1   Overview

This chapter will outline the methodology in carrying out the parametric study on the tow vehicle/caravan combination. The process followed in establishing the geometry profiles of the model which will be used in the CFD study will be discussed along with the CFD parameters which will be evaluated in order to provide the best setup for the initial study and provide a suitable platform for the post modification analysis phase. As this project is predominantly concerned with evaluating the effect that the proposed modifications to the caravan's design has on the overall drag force, the tow vehicle model once established will not be altered in any way.

3.2 Vehicle Selection

As mentioned in section 2.4, the study will utilize the Land Rover Discovery 4 as the tow vehicle. The vehicle was selected due to the availability of data captured through previous studies which would allow for a general comparison between current and previous results. This would also assist in validating the approach used which would be difficult if an arbitrary geometry were utilized instead to represent the tow vehicle.

The geometry and vehicle characteristics have been modelled based on the specifications provided by Land Rover in the Discovery 4 product brochure as detailed in Appendix D.

3.3 Modelling Technique

The initial approach used to generate the model of the tow vehicle involved utilizing the 3D modelling software package PTC Creo Parametric 3.0 to produce the model that would be imported into ANSYS. The reasoning behind the selection of this modelling method was partly due to having familiarity with the program whilst also being able to produce complex geometry features with relative ease. Figure 3.1 depicts the first vehicle model as modelled in Creo Parametric. This model consisted of a body that represented the profile of the LandRover Discovery 4 whilst featuring simplified wheel geometry.

Figure 3.1: Original Land Rover Model (Creo Parametric)

The model was created as a part with a large amount of features which allowed for a close representation of the actual vehicle. The model would be exported to an IGES/STEP file format allowing it to be imported into ANSYS easily. It was noted however that due to the simplified model features predominantly involving the wheels and wheel arches a significant reduction in drag would be obtained which would not truly reflect the actual vehicle. It was noted throughout the research conducted as part of the literature review that wheel arches and external protrusions such as mirrors contribute to the frontal drag profile of the vehicle, therefore it was decided to include these features in the final model.

Figure 3.2 depicts the final geometry which included most of the features that would accurately depict the true configuration of the actual vehicle.
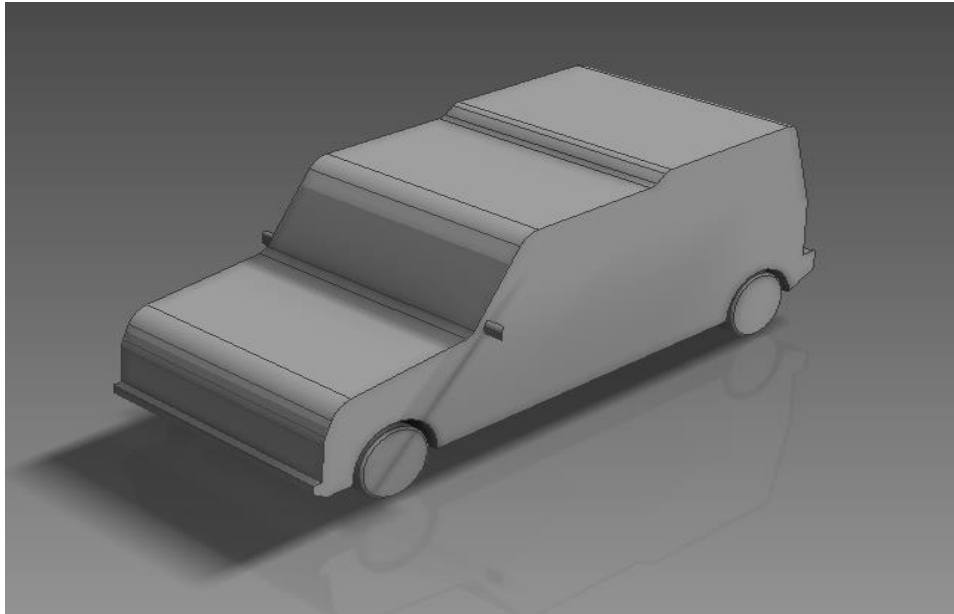
Figure 3.2: Simplified Land Rover Model (Creo Parametric)

The model produced conformed to the Land Rover dimension specifications and allowed for the inclusion of wheel arches, complete wheel and tyre assemblies and side mirrors. It was also noted that this modelling option provided the simplest method of carrying out modifications to a geometry as it is all handled within the same program therefore negating the requirement to learn a new modelling language and conventions It was anticipated that based on the number of ANSYS simulations required and reconfiguration tasks to be conducted, that a portion of time would need to be allocated to exporting and importing geometry which needed to be factored for in the project timelines. It was noted however that a benefit of modelling with an external package allowed the user to perform ANSYS simulation in the background, whilst allowing for modelling work to continue in CREO.

3.4 Vehicle Geometry

The first step in developing the model of the tow vehicle within CREO was to create a rectangular boundary oriented with the x-y plane that would provide the general dimension outline of the vehicle. This would allow for the vehicle to be modelled in proportion to this boundary. The defining dimensions in this first step included; ride height, vehicle length, vehicle height and wheelbase.

The outline of the vehicle was sketched within this boundary and dimensioned accordingly. Once the outline of the vehicle was deemed to be suitable the sketch was then

extruded in the z dimension to a width representing the width of the vehicle minus any extruded features.

Chamfers and blends were then added to the extruded solid to provide a closer representation to the actual vehicle. Wheel arches were added by sketching two circles to the required size and then subsequently cutting material away to a depth that would accommodate the wheels. Once the wheel arches were in place the wheels were added sketched and extruded to the specifications provided by Land Rover.

Once all features were in place an additional reference plane was created and translated to a distance from the sketch face that represented the mid plane of the vehicle. Subsequently all features were mirrored about this plane. Side mirrors were modelled and mirrored about the mid plane completing the vehicle geometry.

Figure 3.3 depicts the model imported into ANSYS Workbench
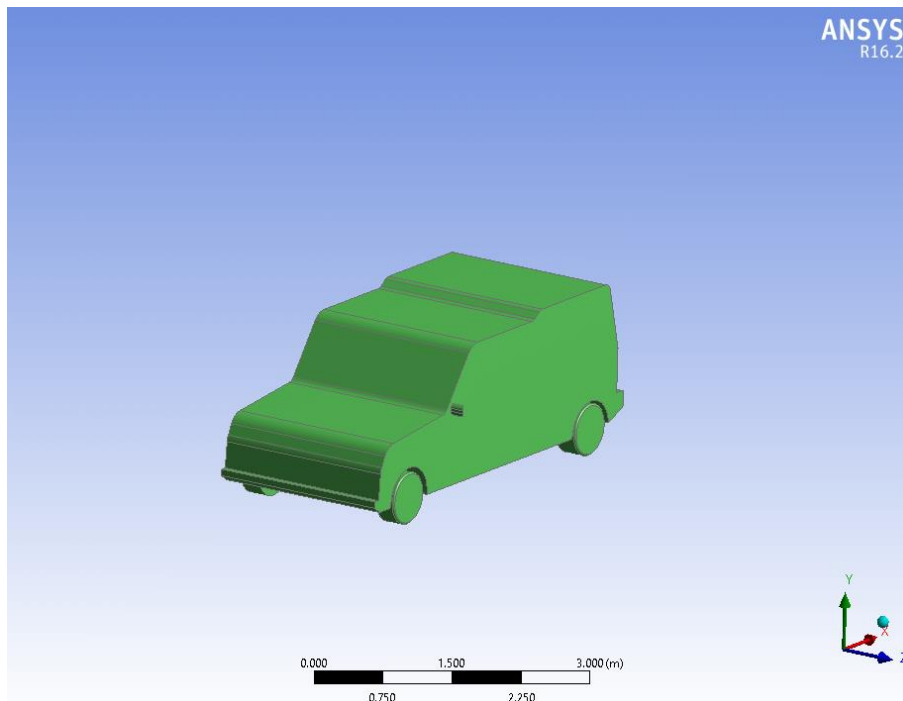
Figure 3.3: Model imported into ANSYS.

An important modelling characteristic to note was that the model was created in its entirety and not represented by half the geometry as was represented in the study conducted by Briskey, 2013. Although it is expected that modelling half the geometry would be satisfactory for a headwind analysis the requirements for undertaking a crosswind analysis

required the entire geometry be modelled to ensure all features of the vehicle are factored into the analysis.

3.5 Fluid Domain

With the geometry of the vehicle established, the fluid body moving around the vehicle required consideration. To simulate a 'wind tunnel' like set up an enclosure around the vehicle was generated. The enclosure was created using the enclosure tool and was subsequently subtracted from the vehicle geometry by using the Boolean tool. The enclosure was set up to allow for enough room forward of the vehicle to allow the airflow to stabilise and with sufficient volume aft of the vehicle to allow for the airflow to re-join and stabilise. The initial enclosure was non-uniform in nature and is represented in Figure 3.4. Further details regarding the experimentation with enclosure size is discussed in section 3.10
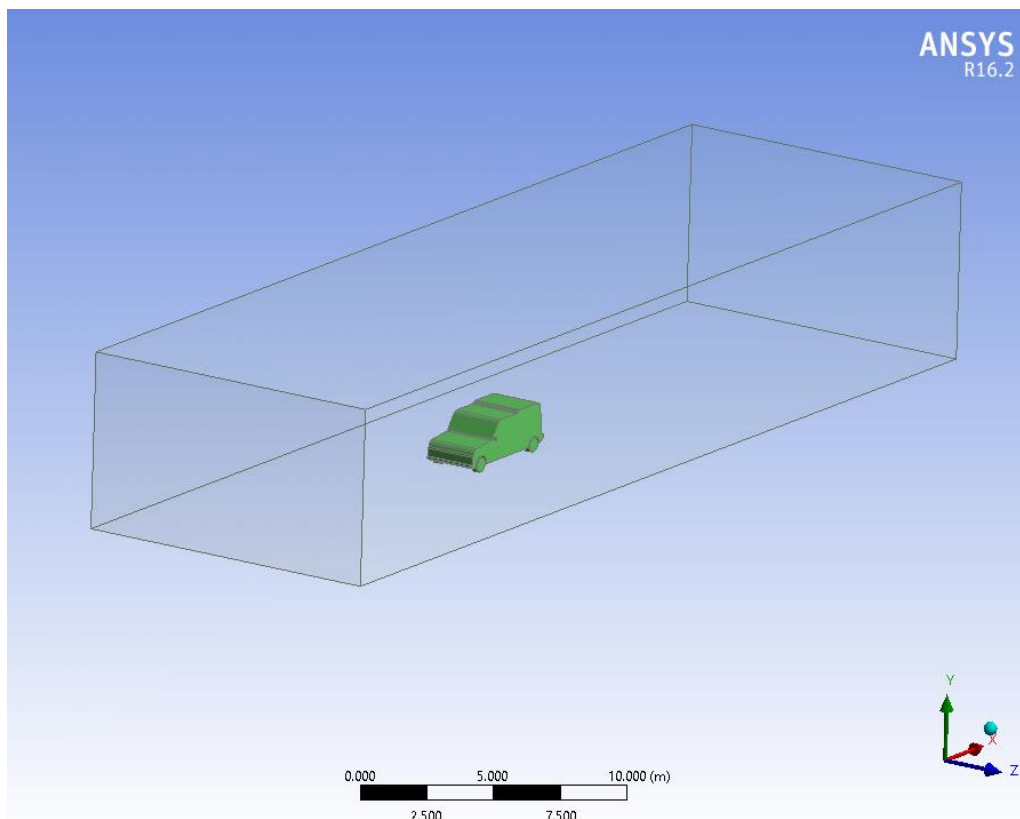
Figure 3.4: Non Uniform Enclosure

3.6 3D Model Validation

In order to assess the validity of the model prior to progressing with the study a set of criteria was established to allow for the model to be considered reasonably similar to the actual vehicle.

The criteria to assess the model against was as follows;

1. Geometric Similarity
2. Coefficient of Drag (Cd)

Due to the technique of modelling the vehicle utilising a certain element of approximation regarding dimensioning, the emphasis was placed on ensuring that the frontal area of the vehicle closely matched the actual vehicle. This was important due to the requirement of using area as a variable in the coefficient of drag equation. Due to the rectangular frontal profile of the 2016 Land Rover Discovery 4 the frontal area was simple to calculate with a high degree of certainty by multiplying vehicle height by the width.

$$A_{frontal} = Height \times Width$$
$$A_{frontal} = 1.92m \times 2.20m$$
$$A_{frontal} = 4.224m^2$$

Once a frontal area value was established a simulation was conducted in CFX with a monitor point set up to identify the drag force in the x-direction on the vehicle body. The velocity of the vehicle for this baseline calculation was set at 80 km/hr (22.22 m/s). Based on the information captured through the literature report, the Land Rover Discovery 4 had a Coefficient of Drag of 0.4. Figure 3.5 depicts the force in the x direction on the surface of the vehicle.
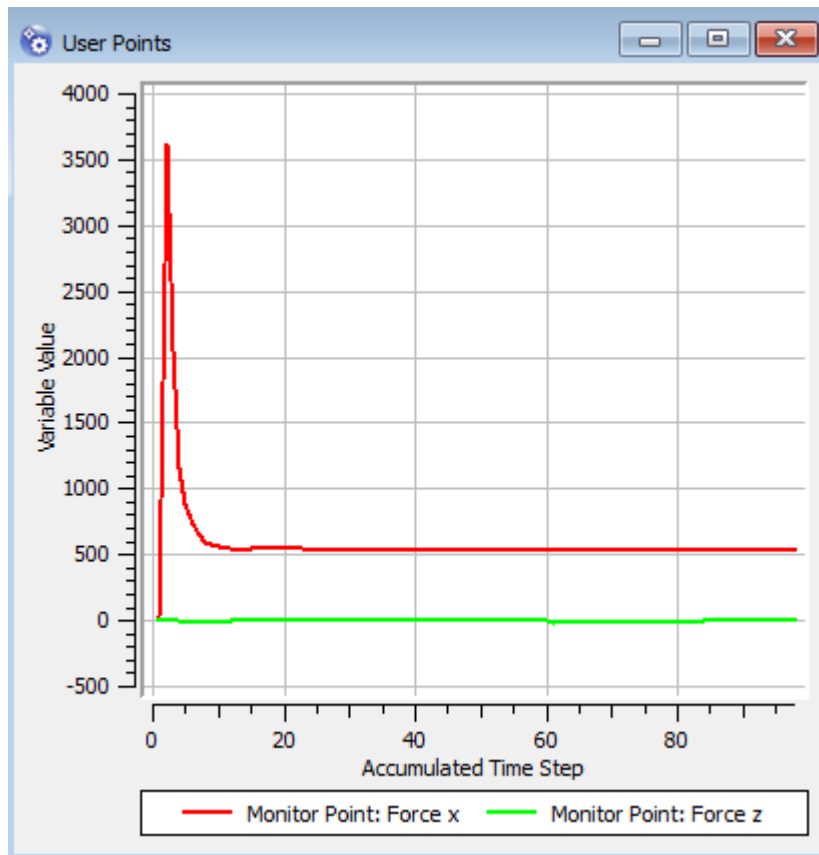
Figure 3.5: Drag Force in X and Z directions on Vehicle

Utilising this value at convergence and inputting into the coefficient of drag equation a baseline Cd was obtained that would provide an indication on how valid the model was in comparison to the actual vehicle. From section 2.4.1 it can be seen that the Coefficient of Drag once calculated was initially determined to be;

$$C_d = \frac{2 \times F_D}{\rho \times v^2 \times A_{frontal}}$$

$$C_d = \frac{2 \times 568N}{1.22kg/m^3 \times (22.22m/s)^2 \times 4.224m^2}$$

$$C_d = 0.45$$

As the Cd figure is approximately 12% greater than the stipulated value provided by Land Rover, it is therefore a valid model to continue the study with. Due to the simplification of

key features an increased coefficient of drag was to be expected. Further alterations to the design of the vehicle were seen to not provide any viable improvement in Cd figure when compared to the effort and time required to alter the model.

3.7 Mesh Setup

Once the initial geometry of the vehicle was created the simulation moved into the meshing phase. It was vital that this process was carried out diligently as the accuracy of any results would be attributed primarily to the quality of the mesh. As the meshing process used is generally tailored towards a particular model or desired outcome it was important to establish a baseline mesh which could be altered in various ways to refine the solution. Once this mesh was deemed appropriate it could be used to undertake a Grid Independence Study were these meshing parameters could be experimented with to validate the solution and more importantly the setup.

As the ANSYS analysis system to be used for this study was CFX, it was important to select the correct Physics and Solver preference from the meshing defaults to suit the study type. The default setting was set as;

Physics Preference: CFD

Solver Preference: CFX

3.8 Global Mesh Sizing Control

Following on from establishing the physics based settings of the mesh, the global mesh sizing controls. The sizing features that would be considered for meshing are; Relevance and Relevance Center, Advanced Size Functions (ASF), Smoothing, Transition & Span Angle Center. For the initial setup it was decided to evaluate the relevance and advanced sizing functions only to allow for a baseline mesh that could be refined even further during the Grid Independence Study as detailed in section 3.9.

3.8.1 Relevance and Relevance Center

The relevance and relevance center are important meshing controls as they allow for the global refinement of the mesh which results in a coarsening of the mesh. By utilising these settings the fineness of the mesh can be easily altered through the use of a sliding scale for relevance and through the selecting between three available settings in Relevance Center.

The relevance sliding scale allows for the adjustment of the mesh between a range of -100 to 100 with 0 being the defaulted value. Moving in a negative direction results in a coarser mesh to begin with which allows for a quicker solution time however the accuracy of the solution is diminished. Moving in a positive direction results in the application of a finer mesh which will provide more accurate results albeit with longer solving times. As the defaulted value is 0 and there are 200 increments to solve for it was decided that any refinement to meshing would be carried out using the Relevance Center thus saving time.

The relevance center simplified the meshing sizing selection process by offering only 3 variables; Coarse, Medium and Fine. For the initial setup of the vehicle it was decided to commence with a medium mesh allowing for further refinements to be carried out in the Grid Independence Study.

3.8.2 Advanced Size Function

The advanced sizing functions allow for the control of meshing growth in critical locations such as curvatures or surfaces. Five options are available for selection; Off, Proximity and Curvature, Curvature, Proximity and Fixed. Off is selected by default. The curvature component of the ASF allows for the mesh to be formed along the edge of a boundary and face with relation to the Curvature Normal Angle hence creating a finer mesh around curves. The proximity feature of allows for the distribution of a defined number of elements into area such as gaps. Figure 3.6 depicts an example geometry with ASF set of Off in comparison to Proximity and Curvature.
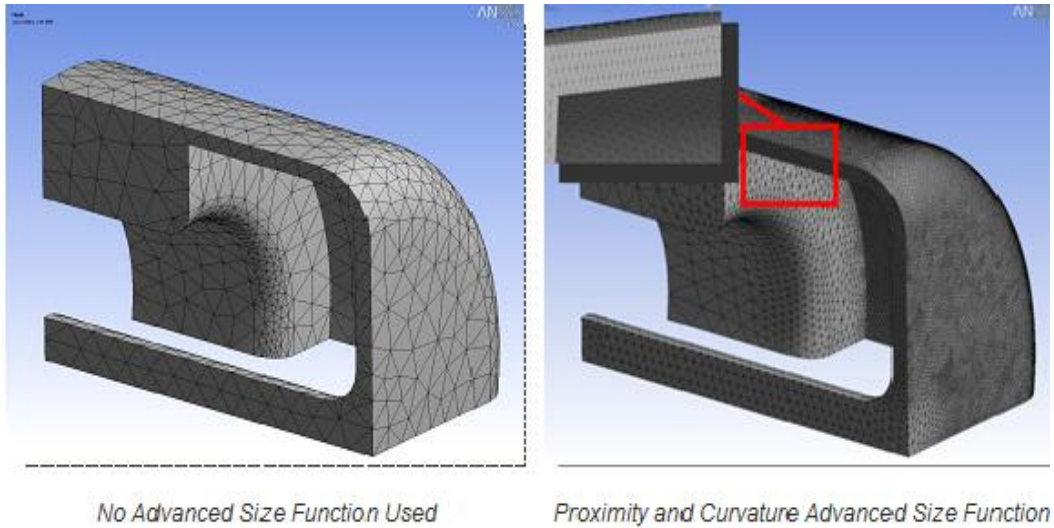
Figure 3.6: ASF Meshing Comparison (Leap Australia, 2011)

For this study the combination of both curvature and proximity would be used as it provided a good balance between mesh detailing at critical locations. Figure 3.7 depicts the mesh around the wheel when the ASF is set to Proximity and Curvature.
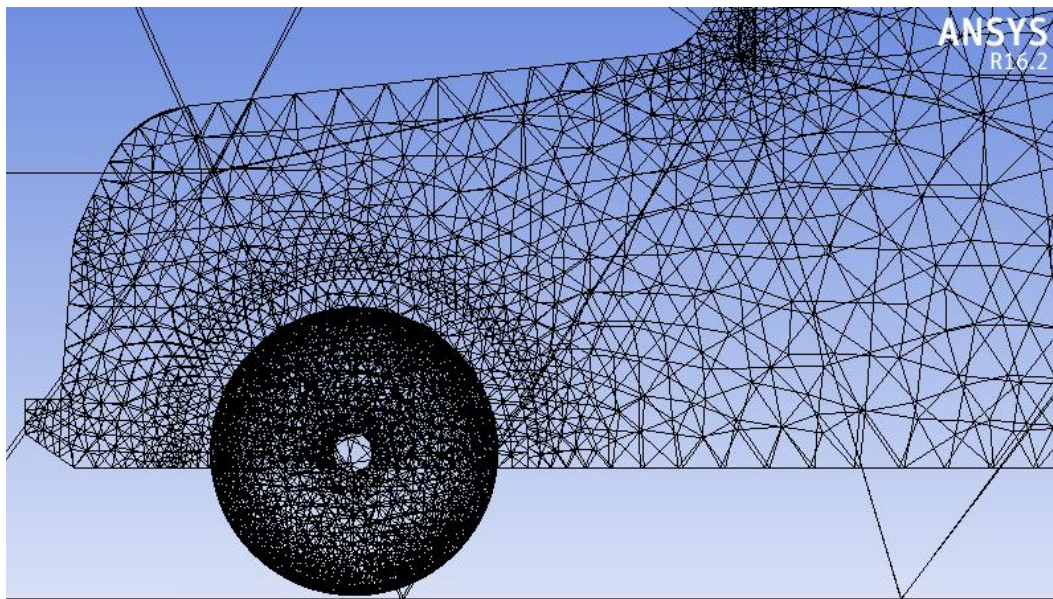
Figure 3-Proximity and Curvature ASF mesh detail

3.8.3 Initial Mesh

The initial mesh setup featured a medium mesh which allowed for a faster solution time in order to validate the vehicle model initially. With the ASF set On: Proximity and Curvature a higher level of detail was maintained at the edge boundaries of the vehicle

with the mesh becoming coarser as it moved away from the edge boundaries. The fluid domain meshing was deemed acceptable at this level of detail as the priority at this stage was ensuring the vehicle boundaries were detailed enough to get a good starting point, prior to refining. At this point it must be noted that the solution time was a large contributing factor to establishing what initial mesh would give an adequate result. Figure 3.8 depicts the initial mesh of the tow vehicle within the enclosure. Figure 3.9 provides a detail view of the initial vehicle mesh.
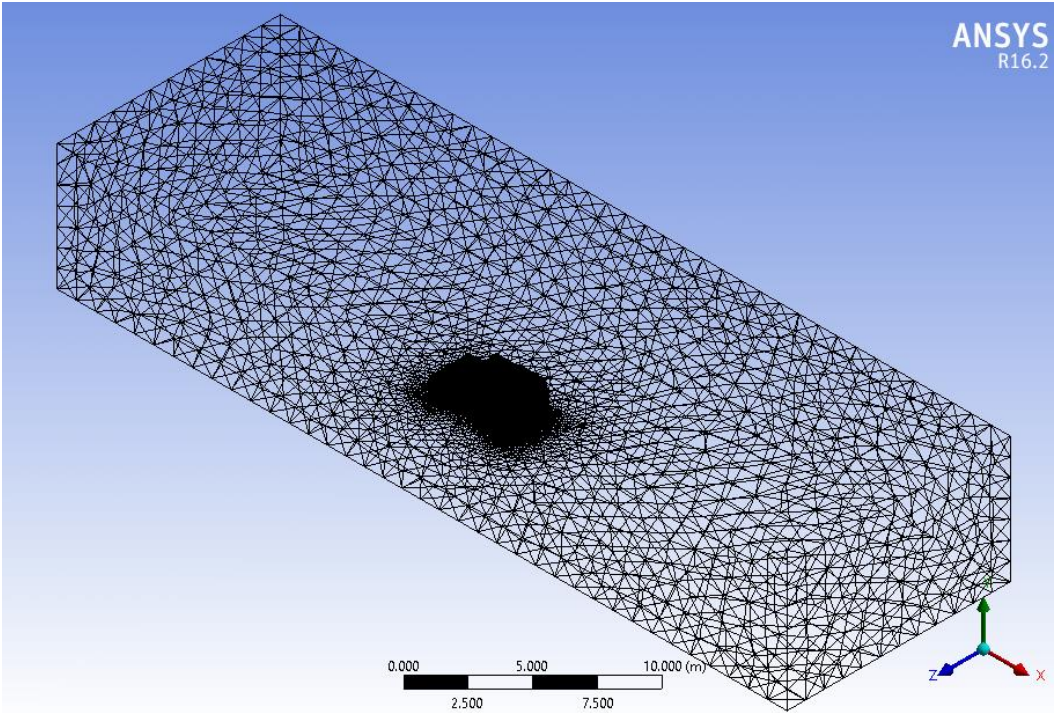
Figure 3.8: Isometric View of Meshed Domain
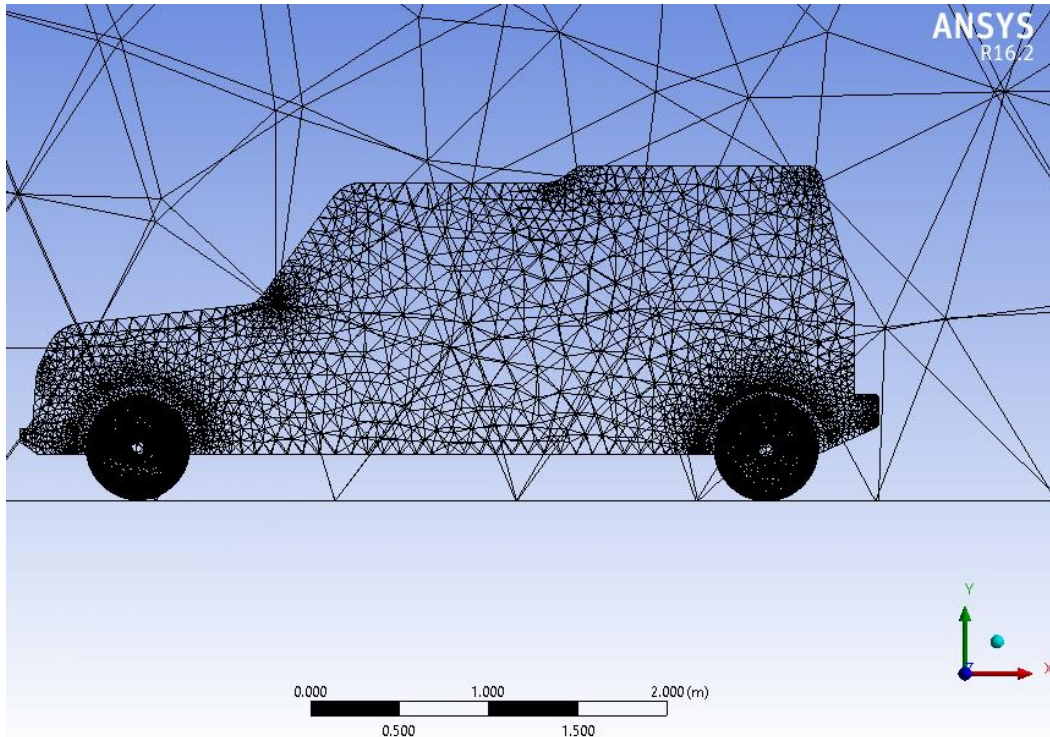
Figure 3.9: Detail View of Initial Vehicle Mesh

3.9 Grid Independence Study

A Grid Independence Study was seen as an important process to ensure that the initial mesh characteristics were suitable prior to applying them to other elements of the study namely the caravan. During the initial run to calculate the Cd of the vehicle, the monitor points for Momentum and Mass being RMS P-Mass, RMS U-mom, RMS V-mom and RMS W-mom in addition to the Turbulence Monitor Points being RMS K-TurbKE and RMS O-TurbFreq, were monitored for convergence based on residual value difference established through CFD literature in the order of 10^{-4}.

When making changes to the mesh detail it is vital that the solver be run to ensure that meshing detail does not affect the validity of the solutions. Once the solution is established with values that are not significantly different to each other it can be decided on a final mesh detail. For the purposes of this mesh independence study the solver was set to 250 iterations. Any solution not achieved by this time step was deemed not converged and as a result the computation time for this study reduced.

The following figures in Table 3 were obtained regarding the meshing detail through the selection of various mesh sizing features in the mesh relevance centre.

Table 3: Relevance

Relevance Centre	Elements	Nodes	Convergence Iterations	Force_x (N)
Land Rover Model				
Coarse	748463	525438	76	568
Medium	1083489	757284	120	569.9
Fine	1309508	911546	86	568

Mesh smoothing aims to improve the quality of the mesh by arranging the location of mesh nodes in relation to surrounding nodes. ANSYS offers three levels of smoothing, these are; Low, Medium and High. As a general rule CFD studies are conducted with a smoothing setting of medium. Table 3 details the results obtained through variation of smoothing settings based on the default CFX meshing settings.

Table 4: Smoothing

Smoothing	Elements	Nodes	Convergence Iterations	Force_x (N)
Land Rover Model				
Low	1297265	902593	113	568.1
Medium	1309508	911546	120	569.9
High	1307431	909915	84	568.6

Transition sizing refers to the rate at which mesh elements grow. There are two control levels that define mesh transition, they are; Slow and Fast. Slow provides a more gradual size transition whereas Fast produces a more rapid and abrupt transition in the mesh. Table 5 details the result variation between both control levels

Table 5: Transition Sizing

Transition	Elements	Nodes	Convergence Iterations	Force_x (N)
Land Rover Model				
Slow	1656797	310443	100	566.03
Fast	574590	120596	99	647.46

Span Angle Centre allows for the control of the mesh refinement based on curvature along the edges. The mesh will elements will subdivide in order to span the distance between edge angles. The three settings available are; Coarse (91º to 60º), Medium (75º to 24º) and Fine (36º to 12º). Table 6 lists the figures obtained.

Table 6: Span Angle Centre

Span Angle Centre	Elements	Nodes	Convergence Iterations	Force_x (N)
Land Rover Model				
Coarse	916072	176032	82	567.4
Medium	988928	189182	136	564.7
Fine	1176190	220867	145	528.6

3.10 Enclosure Dimensioning

An important consideration when establishing the fluid domain around the target vehicle is the enclosure sizing. Due to the configuration of the model being studied the enclosure was initially created with Design Modeller to be a non-uniform bounding box. The dimensions of the original enclosures for the tow vehicle were set as follows;

Table 7: Enclosure Dimensioning

Coordinate	Configuration 1 (m)	Configuration 2 (m)
+X	25	20
-X	15	10
+Y	5	5
-Y	0.001	0.001
+Z	5	10
-Z	5	10
Force x (N)	568	524.2

The enclosure (Configuration 1) was deemed adequate for the study involving the tow vehicle in isolation. When the caravan assembly was imported into the domain, the enclosure automatically adjusted to maintain the same boundary distances.

3.11 Final Mesh Detail

After conducting the grid independence study the following settings were selected for use for the rest of the analysis. The setting selection was based on two competing factors. The first of these was accuracy of the result at convergence. This was compared against the computing resources required as evident in the solution times. In order to proceed with a

setup that would produce the best results given the circumstances an assessment of results was conducted with the final mesh settings in the following table;

Table 8: Mesh Options

Mesh Option	Selection
Defaults:	
Physics Preference	CFD
Solver Preference	CFX
Relevance	0 (default)
Sizing:	
Use advanced size function	On: Proximity and Curvature
Relevance Centre	Medium
Initial Size Seed	Active Assembly
Smoothing	Medium
Transition	Slow
Inflation:	
Use automatic Inflation	None
Inflation Option	Smooth Transition
Transition Ratio	0.77
Maximum layers	5
Growth Rate	1.2
Statistics:	
Nodes	
Elements	
Mesh Metric	None

This mesh was applied to the caravan and tow vehicle configuration with the following mesh dimensions

Nodes: 119876, Elements: 575961

3.12 CFX Simulation Setup

Once a suitable mesh was established through the grid independence study it followed that the tow vehicle and caravan model were imported into the solver and the mesh applied to both entities. The setup of the CFX simulation is detailed in the following section.

3.12.1 Fluid Model Configuration

The fluid properties for use in this analysis are the first critical parameters to set up. As a variety of different atmospheric properties would exist in reality which are linked to various geographic and physical locations it is vital that the CFD study be conducted with fluid properties that would represent an accepted standard ensuring that all results could

be benchmarked against these conditions. The default properties for air were adopted in this case. They are as follows;

Air with temperature of 25ºC

Pressure of 1 atm

Air Density – 1.22 kg/m^3

The other consideration involved selecting the most appropriate fluid model. From the literature review conducted it was decided that the Shear Stress Transport (SST) model was the most appropriate model to use in this analysis as it offered the best accuracy for boundary layer flow.

Transient flow was not considered therefore the solution was set up as a Steady State analysis.

3.12.2 Domain Initialisation

Following the selection of the fluid properties it was necessary to set the initial conditions required for subsequent tests. As the orientation of the model within the domain was set to change to factor in for wind direction, it was necessary that each run was conducted with the correct initial values for the various components of wind.

Initially the straight on test for the purpose of selecting the appropriate mesh was conducted using the wind speed of 80 km/h in the Cartesian direction U which applies to the x axis. The turbulence option was left at the default setting of Medium which set the value (Intensity = 5%).

3.12.3 Boundary Setup

The following tables list the boundary conditions for the analysis in CFX.

Table 9: Inlet Boundary Details

Boundary Feature	Properties
Inlet:	
Type	Inlet
Flow Regime	Subsonic
Mass & Momentum Option	Normal Speed
Normal Speed	80 km/h
Turbulence	Medium (Intensity = 5%)
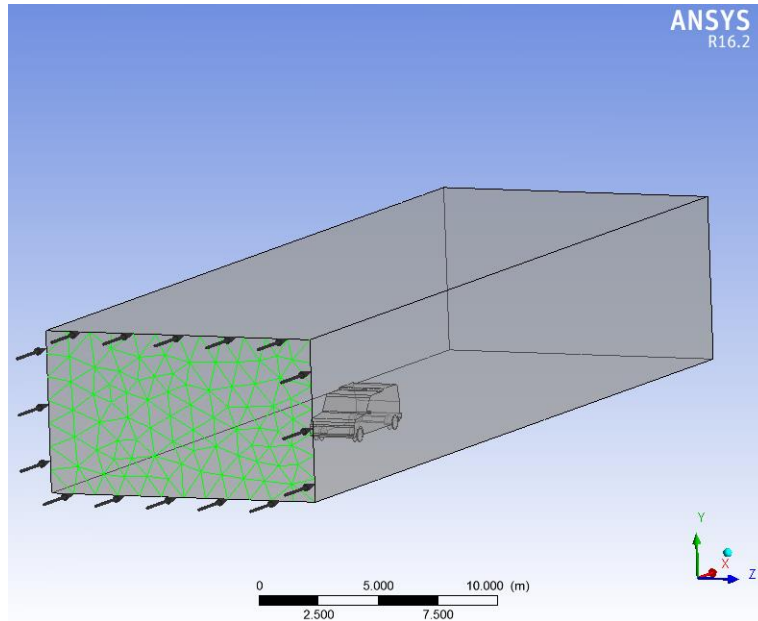
Figure 3.10: Inlet Boundary CFX

Table 10: Outlet Boundary Details

Boundary Feature	Properties
Outlet:	
Type	Outlet
Flow Regime	Subsonic
Mass & Momentum Option	Static Pressure
Relative Pressure	0 Pa
Pres Profile Blend	0.05
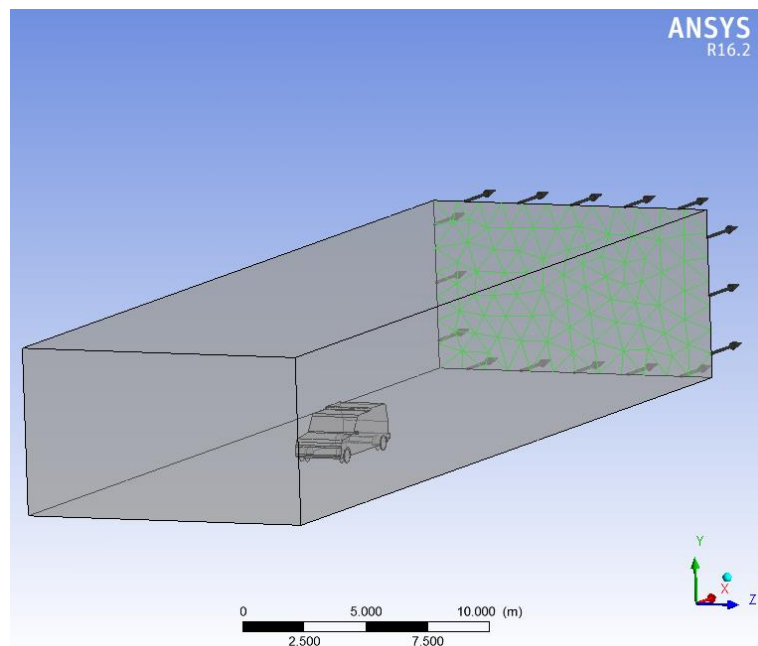
Figure 3.11: Outlet Boundary CFX

Table 11: Opening Boundary Details

Boundary Feature	Properties
Opening:	
Type	Opening
Flow Regime	Subsonic
Mass & Momentum Option	Opening Pres and Dim
Relative Pressure	0 Pa
Flow Direction	Normal to Boundary Condition
Turbulence	Medium (Intensity = 5%)
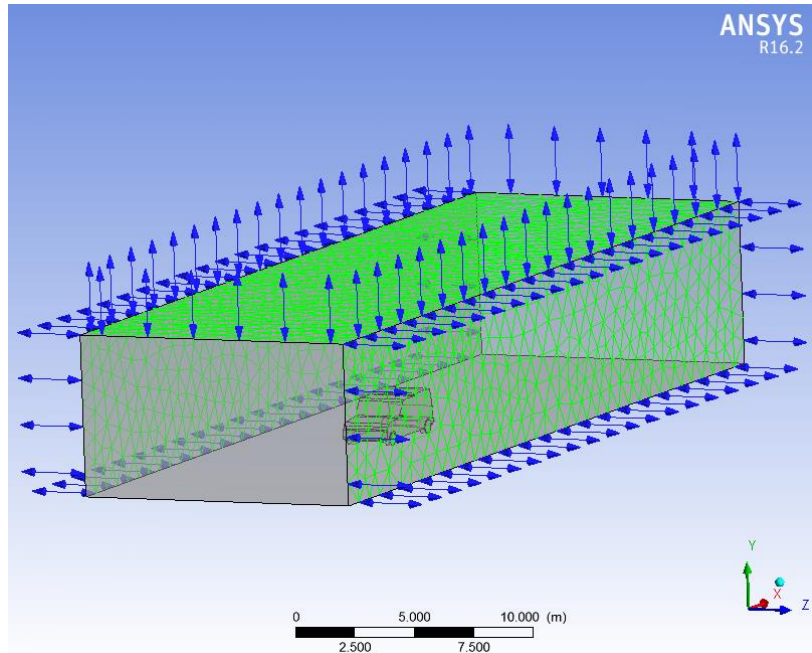
Figure 3.12: Opening Boundary CFX

Table 12: Road Boundary Details

Boundary Feature	Properties
Road:	
Type	Wall
Mass & Momentum	No Slip Wall
Wall Roughness	Smooth Wall

51
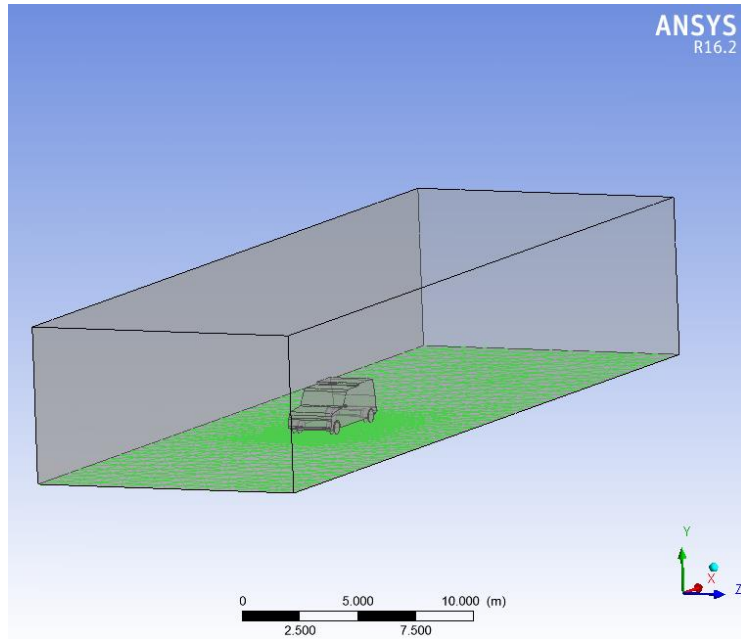
Figure 3.13: Road Boundary CFX
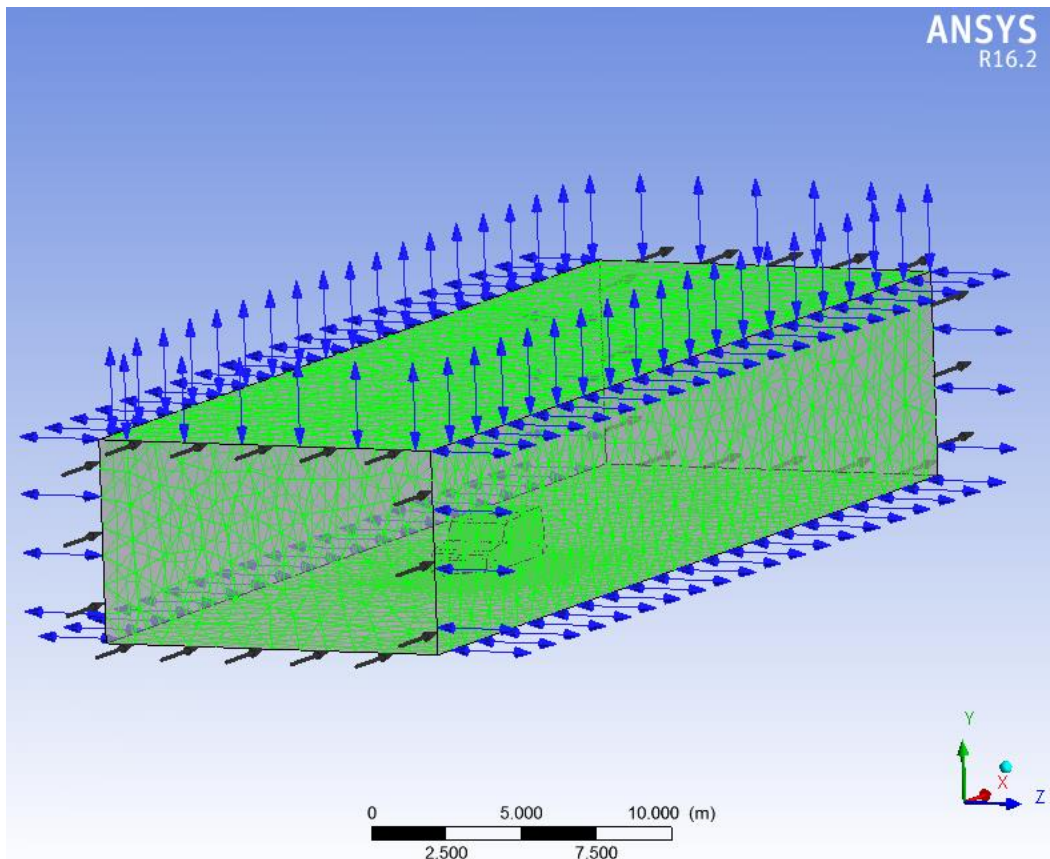
Figure 3.14: Complete Boundary Setup CFX

3.12.4 Monitor Points

User monitor points for frontal drag in x direction set up in CFX Output control as Expression force_x()@Default Domain Default. An additional monitor point used to monitor the drag in the z direction is used in the analysis of crosswind flow. The expression used in this case is force_z()@Default Domain Default. Additional Monitor Point expressions were able to be set to automatically capture key aerodynamic parameters such as coefficients of both lift and drag. It was decided that these additional expressions were not required as the force figures could be used to manually calculate the subsequent Coefficient of Drag values with little effort.

3.12.5 Solver Control Setup

The Solver Control Setup settings with CFX-Pre allow for setup of key simulation parameters

Table 13: Solver Control Details

Solver Control Basic Settings	Settings
Advection Scheme Option	High Resolution
Turbulence Numerics Option	First Order
Minimum Iterations	1
Maximum Iterations	250
Timescale Control	Auto Timescale
Length Scale Option	Conservative
Timescale Factor	2
Residual Type	RMS
Residual Target	1.E-4

3.12.6 Solution Component Setup

In order to maximise the processing power of the computer hardware used for the CFD Analysis some specific settings can be chosen that will utilise the maximum potential of the computing system. The processor used for this study is the Athlon X2 245 with a clock speed of 2.9 GHz. The processor has dual core capability allowing it to simultaneously utilise both cores to perform CFD computations as well as manage computer background tasks.

When defining the run, the selection Platform MPI Local Parallel was made. This utilised 2 partitions to perform the run.
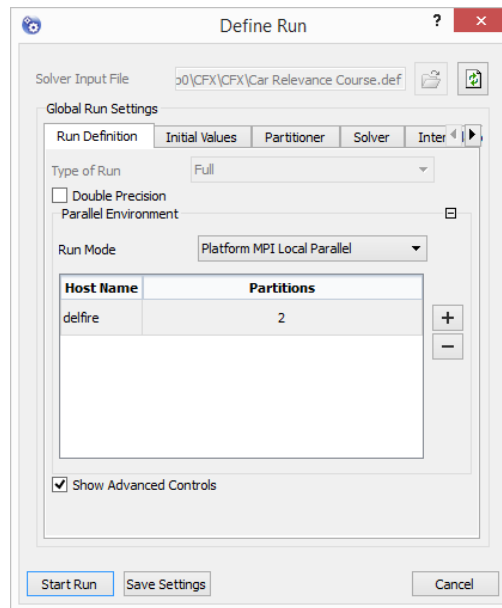
Figure 3.15: Solver Run Settings

3.13 Caravan Selection

Without the provision of a caravan model to utilise in this study by way of a project sponsor, it was necessary to select a caravan design and produce a model for use in the study. After a review of literature the design to be analysed was based around a combination of features as displayed by the following three caravan models. They are;

- Jayco Starcraft
- Trakmaster Simpson
- Majestic Knight

The final caravan model as produced in CREO provided an average representation of all three caravan models researched.

Figure 3.16: Jayco Starcraft (Jayco, 2016)

Figure 3.17: Trackmaster Simpson (Trackmaster, 2016)

Figure 3.18: Majestic Knight (Majestic Caravans, 2016)

3.13.1 Caravan Geometry

The dimensioning for the caravan was based off the Jayco Starcraft with a length of 5.33 m, width of 2.3 m and a height of 2.89 m. The caravan features a standard draw bar length of 1.8m and travels upon on a twin axle wheeled arrangement.

The caravan was modelled by starting with a rectangle to provide the boundary for the external geometry. From here the outline was drawn and then extruded to the required width. The wheel arched were drawn and then extruded using the remove material function. The wheels were subsequently modelled and finally the drawbar 'A-Frame' was modelled. When all the major components were modelled some chamfers and rounds were added to the frontal profile of the caravan. The model was added to the LandRover model and saved as an assembly file. From here the assembly was exported to IGES format for use within ANSYS. Figure 3.19 depicts both the front and side profile of the modelled caravan.
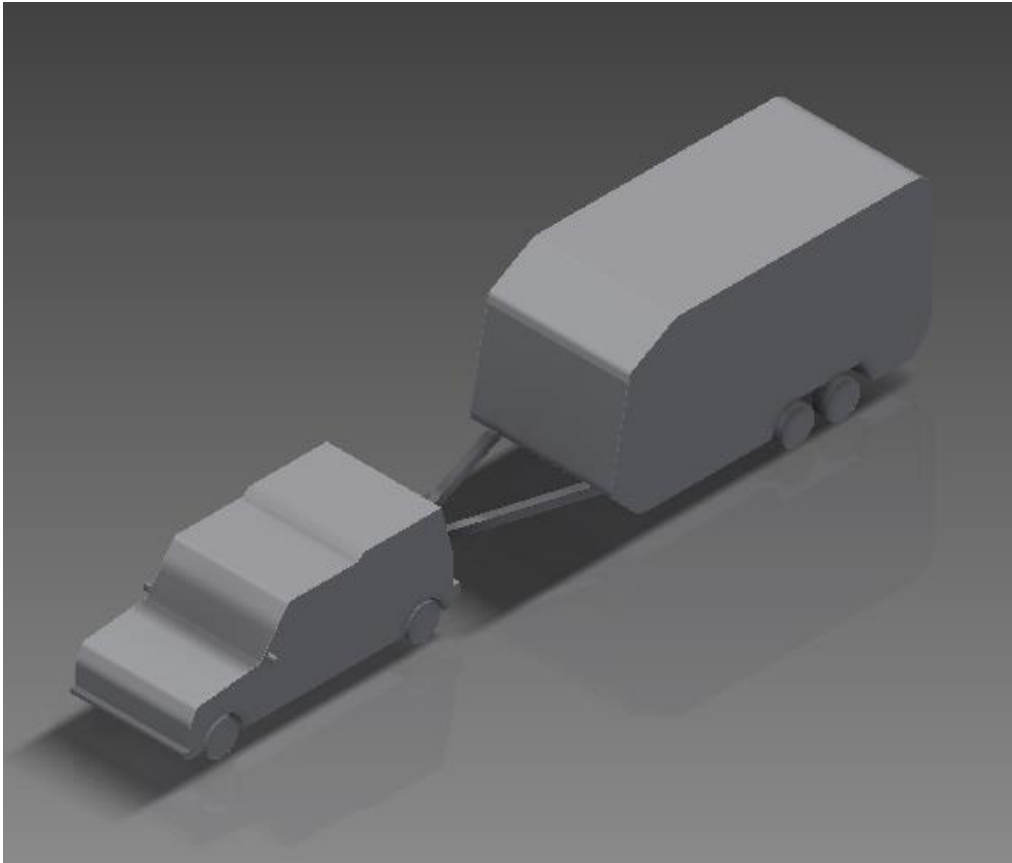
Figure 3.19: Final Caravan Model

3.13.2 Caravan Meshing

Given the similarity in some of the caravan geometry to that of the tow vehicle it was decided to commence the study with the same mesh as was used in the tow vehicle. This also ensured that the features of the caravan such as wheels and wheel arches retained a higher quality mesh without featuring a very large number of elements which would subsequently extend the computation time. Figure 3.20 depicts the final mesh used for the caravan assembly.
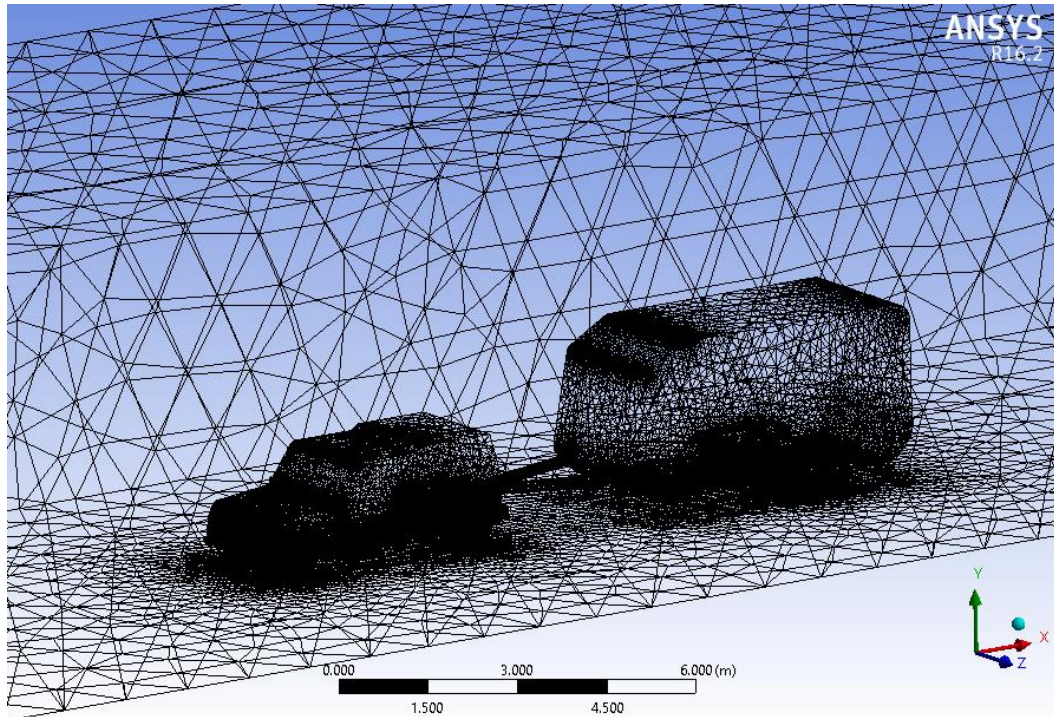
Figure 4: Car & Caravan Model Mesh

The model was rotated within the enclosure to reflect the wind direction and then the simulations were carried out. It was noted that with simulating wind impingement angles of less than 30º the solutions took very long to converge and in some cases did not converge at all. The transition sizing was changed to fast for investigation and some observations regarding convergence that altered the mesh for the combined assembly.

Firstly, the solution converged with very minor imbalances in the RMS residuals. Secondly convergence occurred in approximately 50% of the iterations required by the slower transition mesh. Finally when comparing the results between both converged solutions the difference in monitor point results was generally in the vicinity of being under 1% different. It was therefore decided that in the interest of keeping computation time to a minimum given time and physical resources that this error could be considered reasonable and allow the pre-optimization and parametric study to continue.

3.14 Caravan CFX Simulation

From force monitor point image – Force measured as 1436 N

The Coefficient of Drag for the combined test model was calculated by;

$$C_d = \frac{2 \times F_D}{\rho \times v^2 \times A_{frontal}}$$

$$C_d = \frac{2 \times 1436N}{1.22kg/m^3 \times (22.22m/s)^2 \times 6.65m^2}$$

$$C_d = 0.72$$
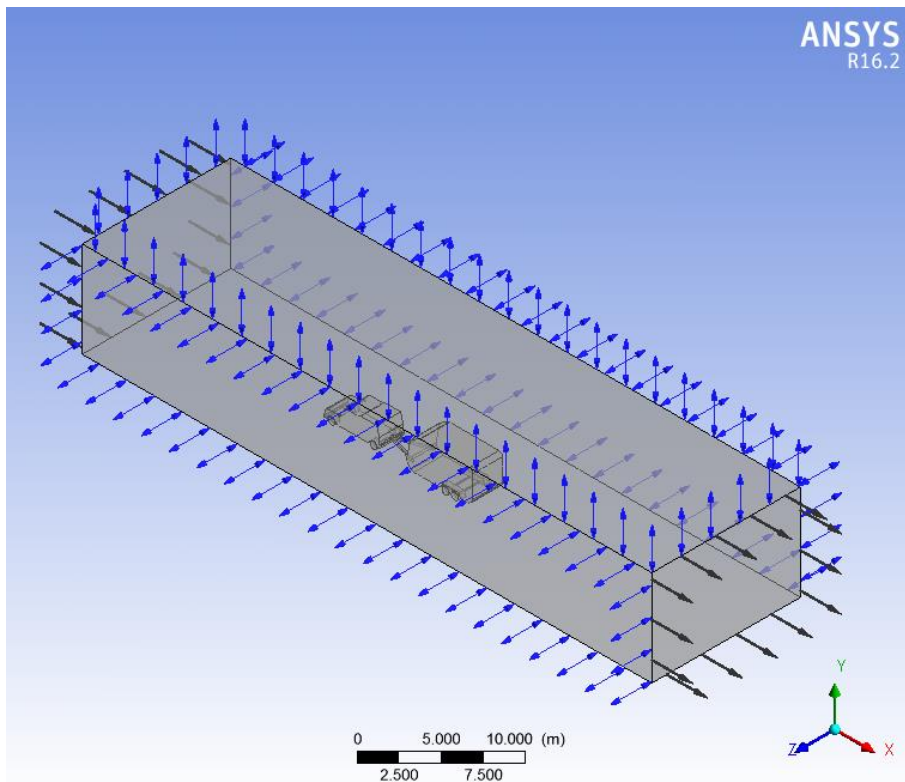
Figure 3.21: Car Caravan Boundary Set Up at Zero Yaw
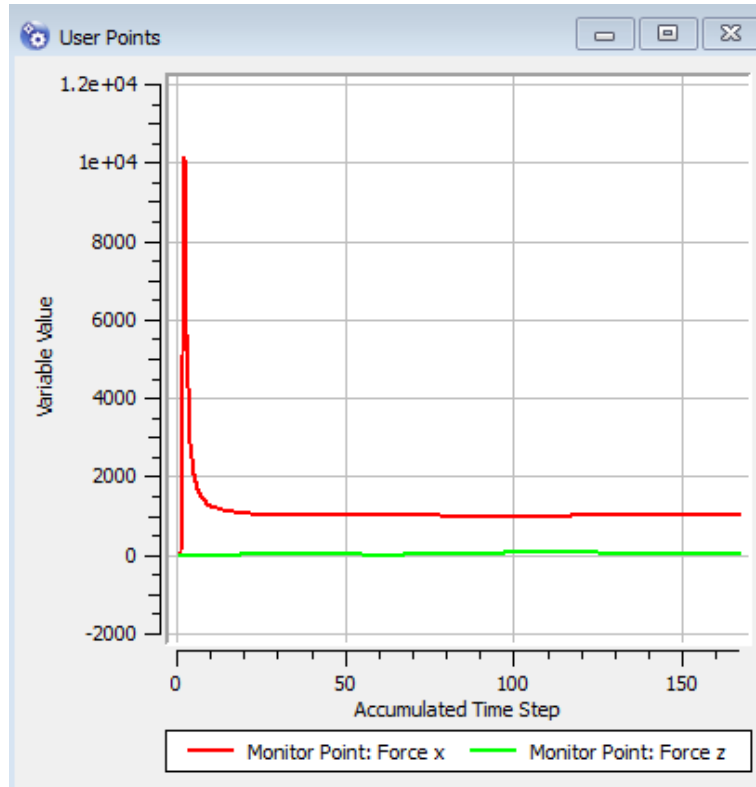
Figure 3.22: Force Monitors Graph for Baseline Caravan
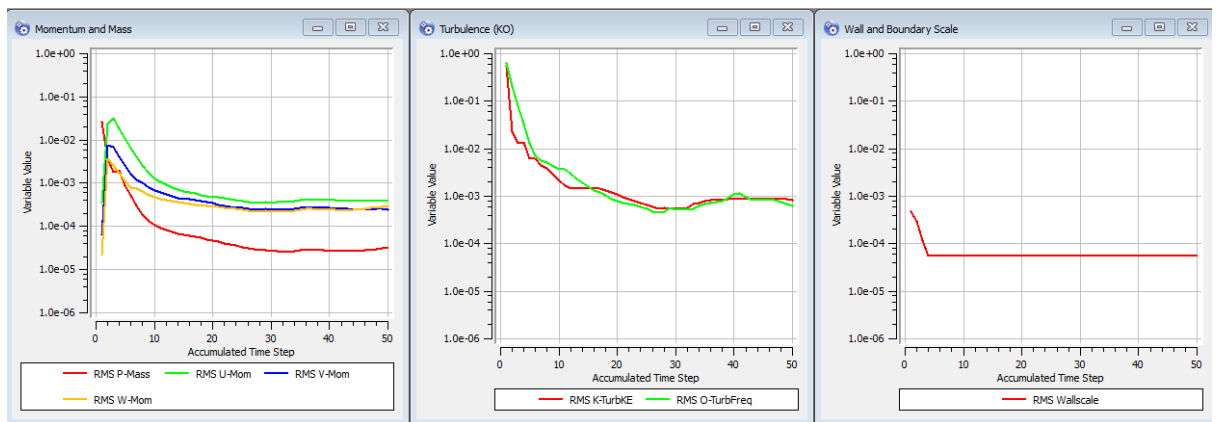
Figure 3.23: Residuals-At convergence (Caravan Set Up)

3.15 Summary of Results

LandRover Discovery 4 model produced 568 N of drag force in x direction. Fuel consumption figure from OEM specifications of 8.8 L/100km (Combined). For the purposes of this study the increase in drag force produced by the caravan will be divided by the Landrover force and then used to extrapolate fuel economy figures.

Given a force of 1436 N produced in the tow vehicle caravan combination, then preliminary fuel consumption for the vehicle when towing the baseline configuration caravan will be;

2.52×8.8

$= 22.2$ L/100 Km

CHAPTER 4 – PRE-OPTIMIZATION STUDY

A study was conducted on the car and caravan combination prior to modification in order to gather some initial data. This data would be compared against post modification results to ascertain whether any advantages could be gained from implementing the modification to the baseline configuration.

The first part of this study involves verifying the flow patterns that are present around the tow vehicle and caravan combination in various cross wind configurations and the forces at play on the vehicles in a static set up. The configurations for the tests were as follows;

Wind Speed varied of values 50, 80 and 100 km/h

Relative Wind Vector Angles of 0,15,30,45 & 60 degrees.

The major quantitative areas of interest that can be used to make an informed qualitative assessment of the flow patterns and aerodynamics of the caravan include the following;

- Flow Velocity
- Forces in X, Y and Z coordinates
- Turbulent Kinetic Energy
- Pressure Gradients

The car and caravan combination was simulated under the flow conditions detailed above and the following initial results were obtained. These results would be used for comparison during the parametric study detailed in Chapter 5.

4.1 Wind Loading Forces

By setting up monitor points to record the forces experienced on the models surfaces in three dimensions it is possible to make some observations regarding the effect wind speed and wind angle have on the car and caravan. The following graphs represent the forces in their respective dimensions. The data for these graphs is located in Appendix E.

4.1.1 Drag Force in X Direction
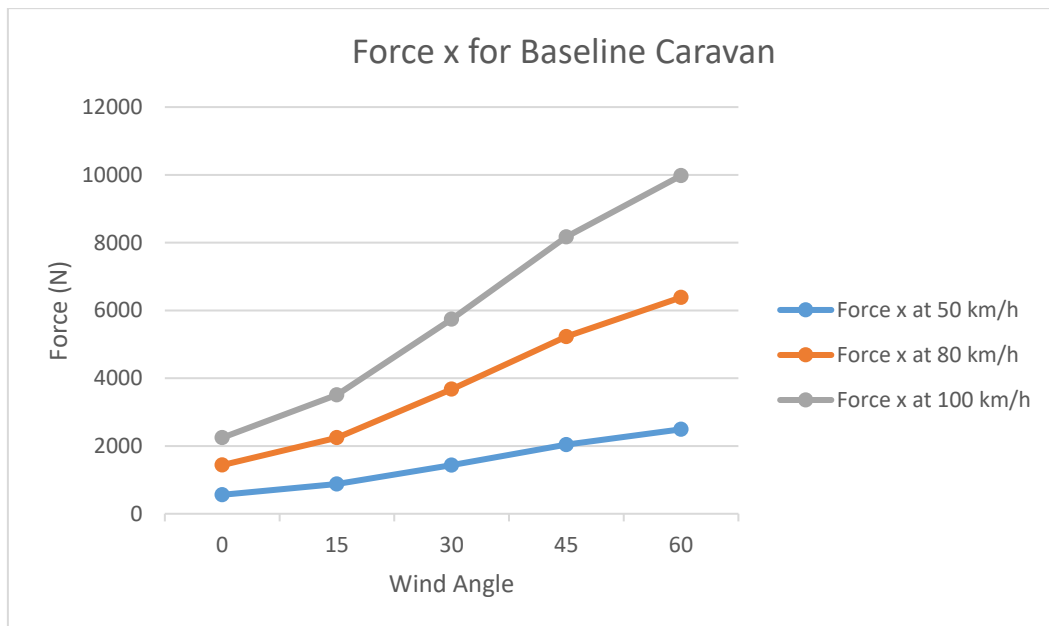
Figure 4.1: Force in X Direction for Baseline Caravan

It can be observed that as the velocity of the wind flow increases the forces produced increase exponentially, this can be attributed to the kinetic energy relationship with the force produce at double the velocity being 4 times as great.

As the model is rotated within the flow the forces in the x direction increase. It is noted that the rotation angles between 15 and 45 degrees show the greatest increase in force produced. This can be attributed to the side of the model coming into play presenting itself to the airflow

4.1.2 Lift Force in Y Direction
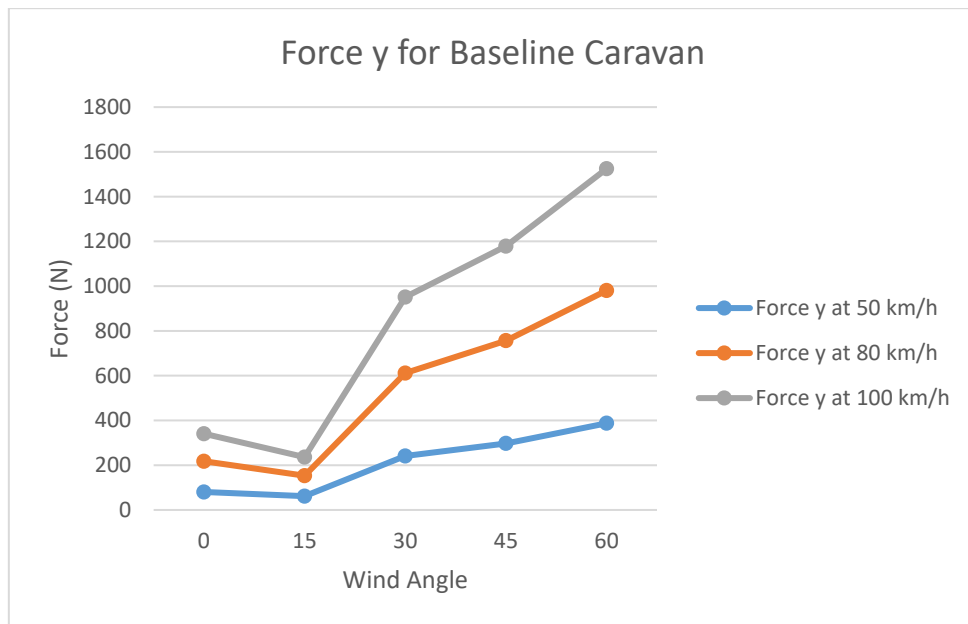
Figure 4.2: Force in Y Direction for Baseline Caravan

As with the force in the x direction it can be also seen that as the velocity increases the force is seen to increase as is expected from the kinetic energy equation relationship. As the caravan is rotated to orient itself 15° into the flow it can be seen that the force decreases slightly until the caravan is rotated to the 30° angle where it increases steadily.

The increase in lift forces can be attributed to the exposure of leading edges to the flow as the caravan rotates through to 60° rotation. These leading edges are generally rounded and increase the velocity of the fluid flowing over them as is seen with the front roof section of the caravan.

4.1.3 Side Force in Z Direction

As the wind angle is altered from 0° through to 30° it can be seen from the data collected that the force increases rapidly due to a greater surface area being presented to the flow.

As the angle increases past 30° and through to 60 degrees the opening between the caravan and the car plays a large role in reducing the forces as the flow passes between the vehicles with lesser obstruction.
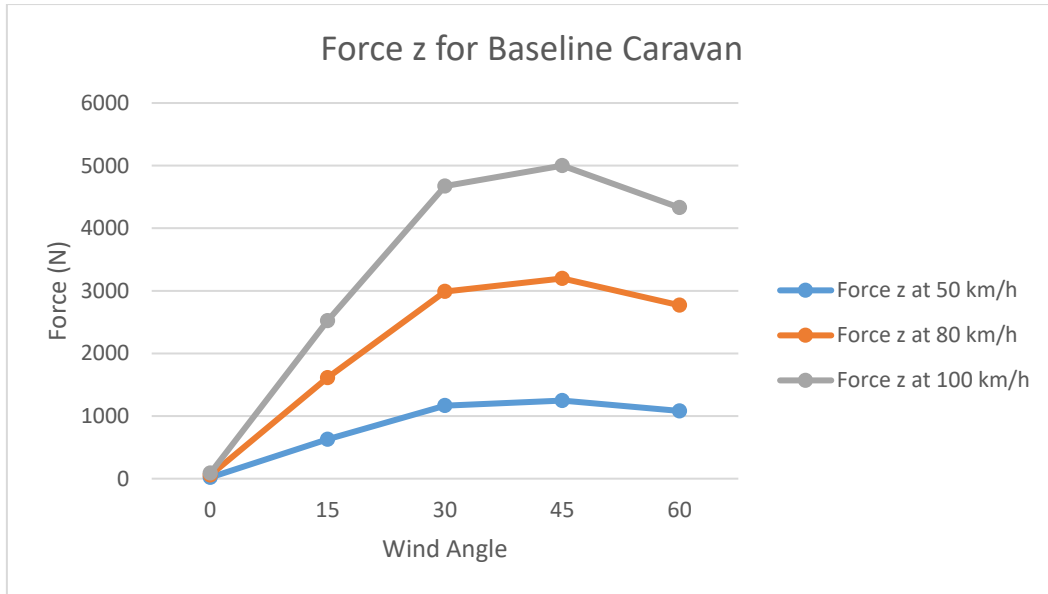
Figure 4.3: Force in Z Direction for Baseline Caravan

4.1.4 Flow Streamlines

The baseline caravan was simulated at 80 km/h wind speed with the following streamline plot produced. The flow makes its way over the bonnet of the car increasing in velocity as it passes over the rounded bonnet and roof. As the flow makes its way to the rear of the vehicle a portion of the flow strikes the front of the caravan and begins to circulate in the vehicle/caravan gap. The remainder of the flow can be seen to travel across the top of the caravan, increasing in velocity as it passes of the upper leading edge and rear trailing edge where it re-joins the airflow around the periphery of the caravan.

It is also observed that the air entering the wheel arches exits with a rotational flow profile.
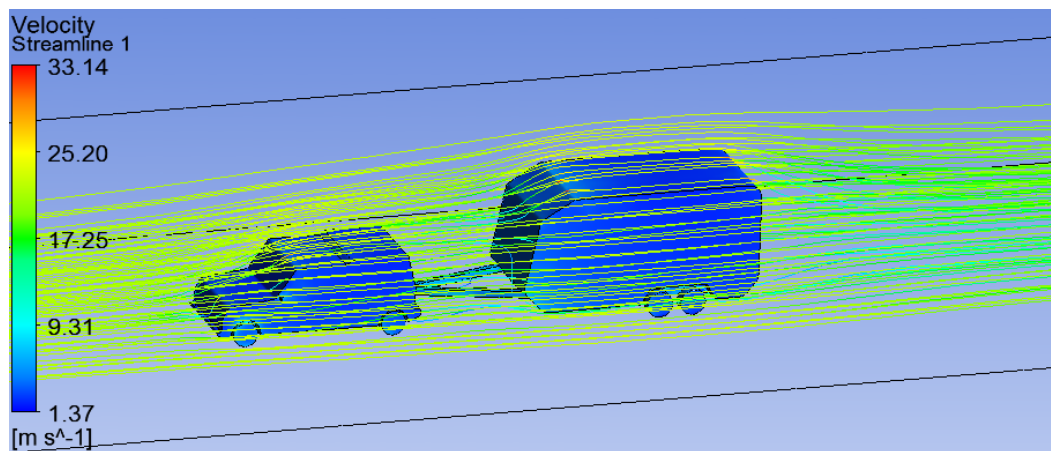
Figure 4.4: Velocity Streamlines for Baseline Caravan

65
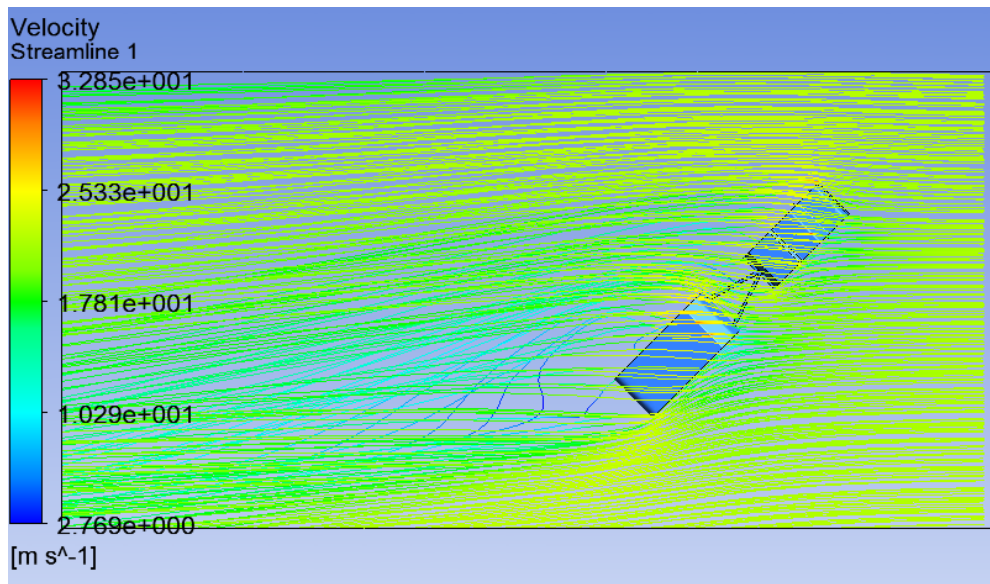
Figure 4.5: Velocity Streamlines Baseline Caravan at 45° flow (1)
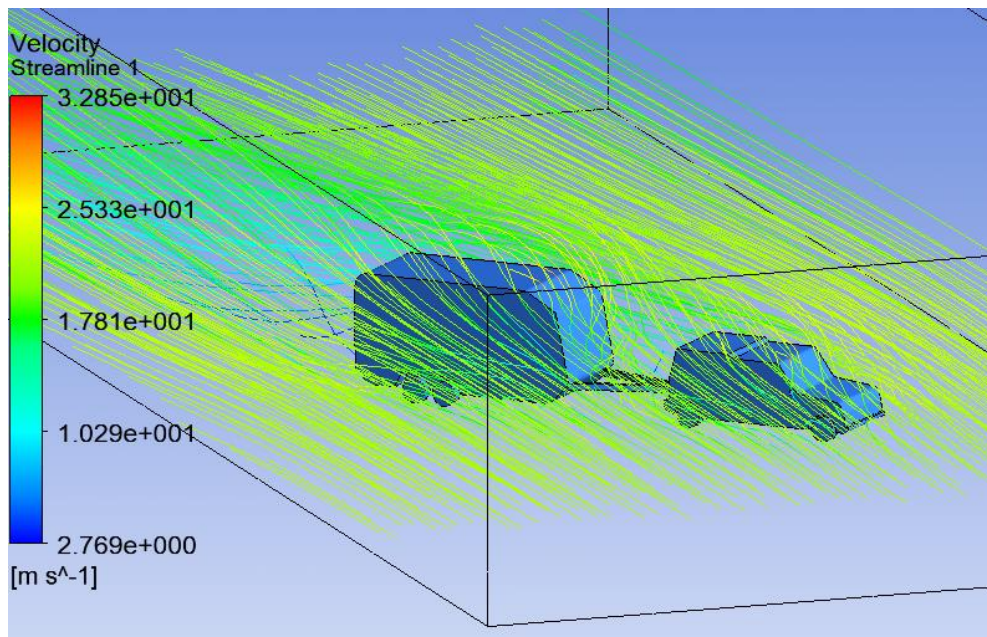
Figure 4.6: Velocity Streamlines Baseline Caravan 45° flow (2)

When the caravan is rotated into the wind the flow impinges on the side wall of the caravan producing side forces on the caravan. Air flow also makes its way between the car and the caravan and spills over the leeward edge of the caravan where it becomes detached from the side of the caravan. The airflow subsequently begins to swirl as travels downwind past the rear of the caravan. The detachment becomes more pronounced as the wind angle increases.

66

4.1.5 Pressure Distribution

At a wind velocity of 80 km/h the maximum pressure value of 304 Pa is observed to be located at three key locations, these are; front vehicle air dam, vehicle windshield and front of the caravan. As the wind angle changes the maximum pressure value location moves across and around the side front quarter of both the vehicle and the caravan.
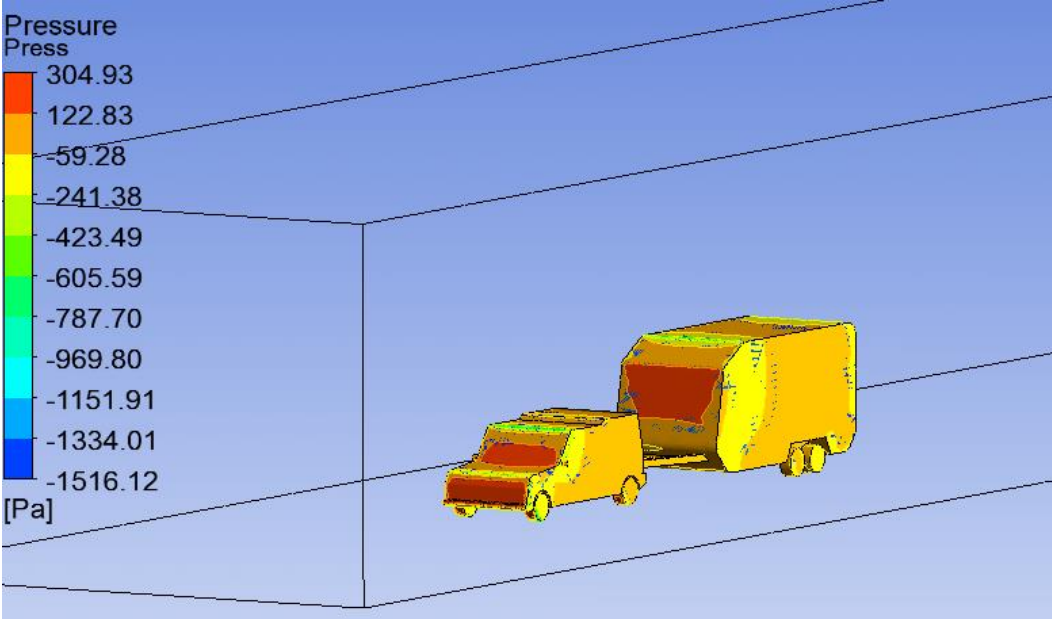
Figure 4.7: Pressure Distribution for Baseline Caravan at 0° flow
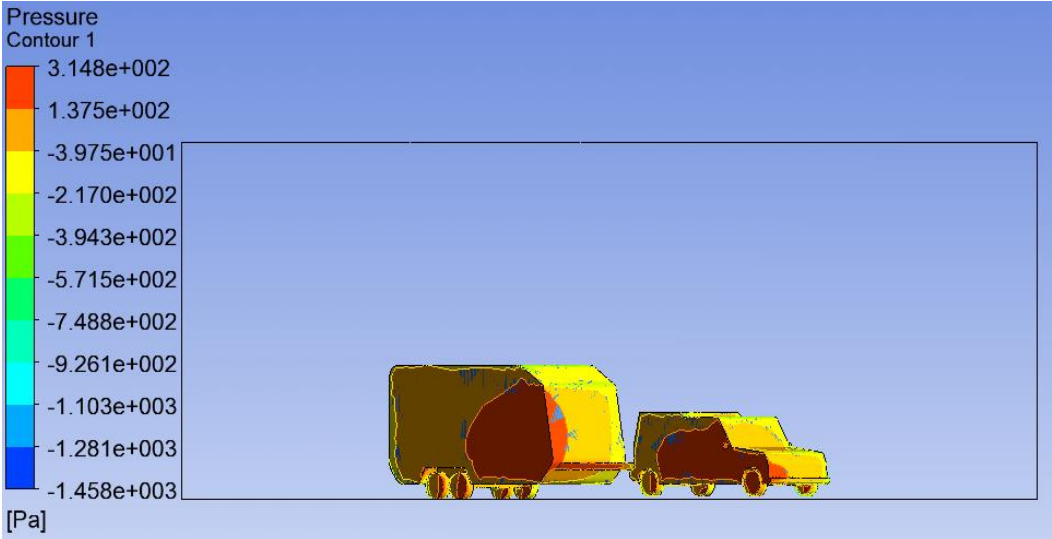
Figure 4.8: Pressure Distribution for Baseline Caravan at 45° flow

4.1.6 Turbulence Kinetic Energy

As the air flows around the profile of the caravan it loses some of its momentum as it moves past certain features such as the wheels and sharp edges of the caravan body. As the airflow begins to swirl forming eddies and continues changing its direction and magnitude, it becomes turbulent. The turbulence intensity is related to its kinetic energy and the Turbulence Kinetic Energy (TKE) provides a numerical value for this energy.

Simulations on the baseline caravan configuration in a zero yaw condition show when plotted areas of turbulent airflow at the following locations;

- gap between car and caravan
- front side edges of caravan
- wheels
- rear of the caravan
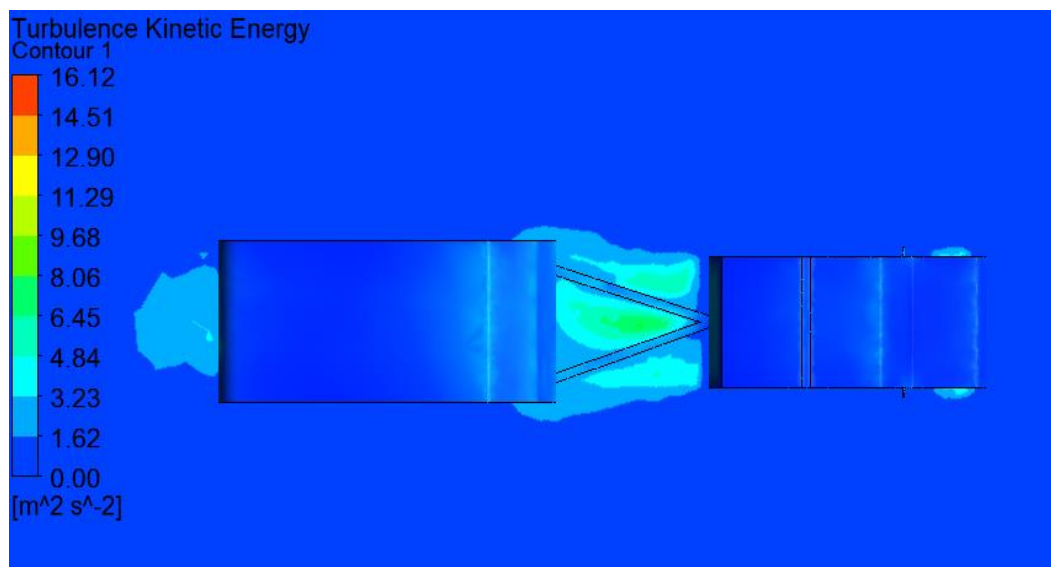
Figure 4.9: Turbulent Kinetic Energy for Baseline Caravan at 0° Yaw

As the caravan is rotated into the flow the turbulent flow increases in magnitude and also extends out past the leeward side of the car and caravan. It can also be observed that the turbulent kinetic energy is higher at the leeward side surface of the model.
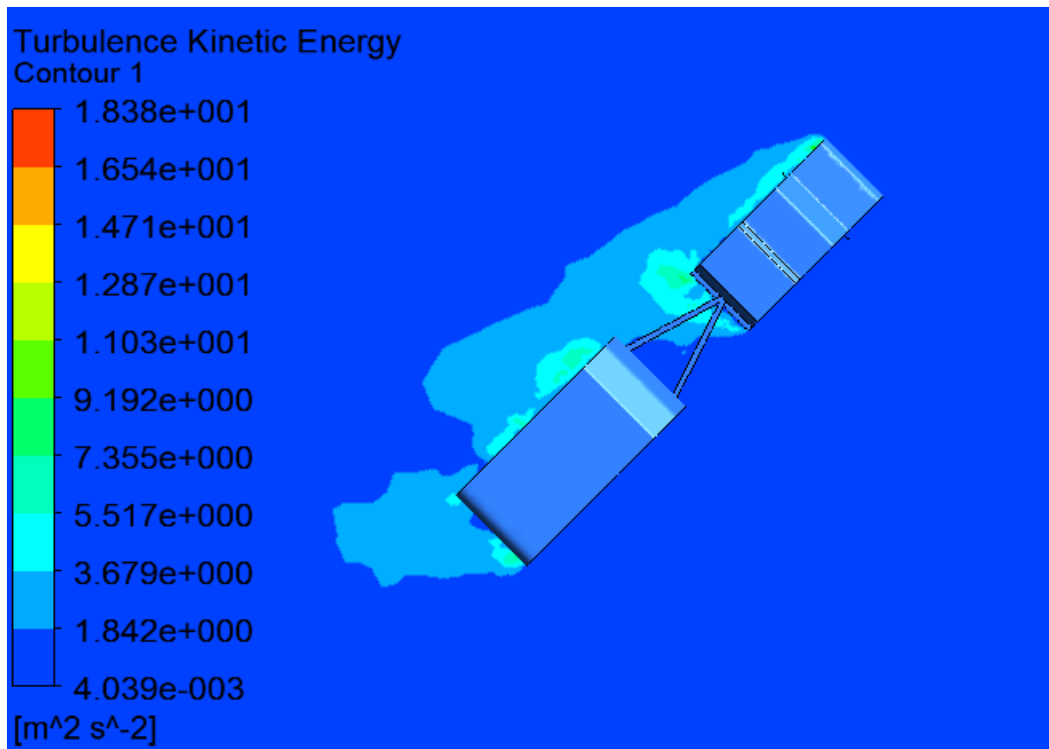
Figure 4.10: Turbulent Kinetic Energy for Baseline Caravan at 45° Yaw

CHAPTER 5 – PARAMETRIC STUDY

5.1 Overview

Following the pre-optimization study and collation of data the study moved into the parametric study phase were modifications would be conducted to the baseline design and the test vehicle combination reassessed through CFD for any drag reductions that may be on offer.

As the study is primarily concerned with the effect of a crosswind flow imposed on the caravan at an angle relative to direction of travel it was decided early on that any modifications explored would be concentrated along the lateral periphery of the caravan, and any areas that were notorious for crosswind air disturbances as encountered during the review of existing literature.

The areas of focus included;

- Gap between Tow Vehicle and Caravan
- Caravan Drawbar
- Caravan Edge Profile
- Caravan Front Profile

5.1.1 Car and Caravan Gap

A simple approach to reducing the gap between the car and the caravan is to reduce the length of the draw bar. It was decided that although reducing the draw bar length would have an impact of the manoeuvrability of the caravan when being towed about, it was worthy of being explored for the purposes of purely carrying out an aerodynamic analysis.

The draw bar was shortened from the standard 1.8m length to 1.5m and 1.0m. It was encountered during the literature review that there is merit in exploring the effect that reducing the draw bar length would have on the forces experienced by the caravan.

No other physical modifications would be performed on the draw bar other than altering the length from the hitch point to centreline of the caravan.

5.1.2 Caravan Edge Profile

The second area of the caravan's geometry that was modified was the edge profile of the caravan's side and front profile. The baseline caravan was modelled with sharp perpendicular corners. Upon researching various caravan models during the literature review it was noted that caravans generally do not have much in the way of curvature around the edges.

The two edge profiles that are explored in this study are;

- 100 mm radius
- 350 mm radius

It was decided to select these dimensions based on the aggressiveness of the curvature starting with a 100 mm mild curvature and then progressing up to the more aggressive 350 mm radius.

It was decided that for the wheel arches, the same radiuses would apply. It was noted however that the 350mm radius was not geometrically accurate when used in this area. It was decided to utilise the 100 mm curvature for this area.
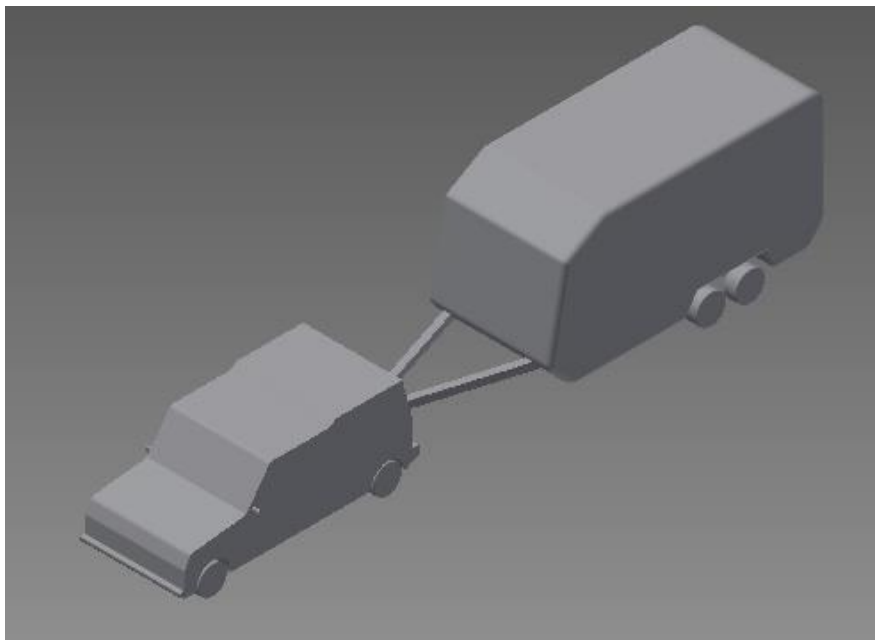
Figure 5.1: 100mm Caravan Edge Radius
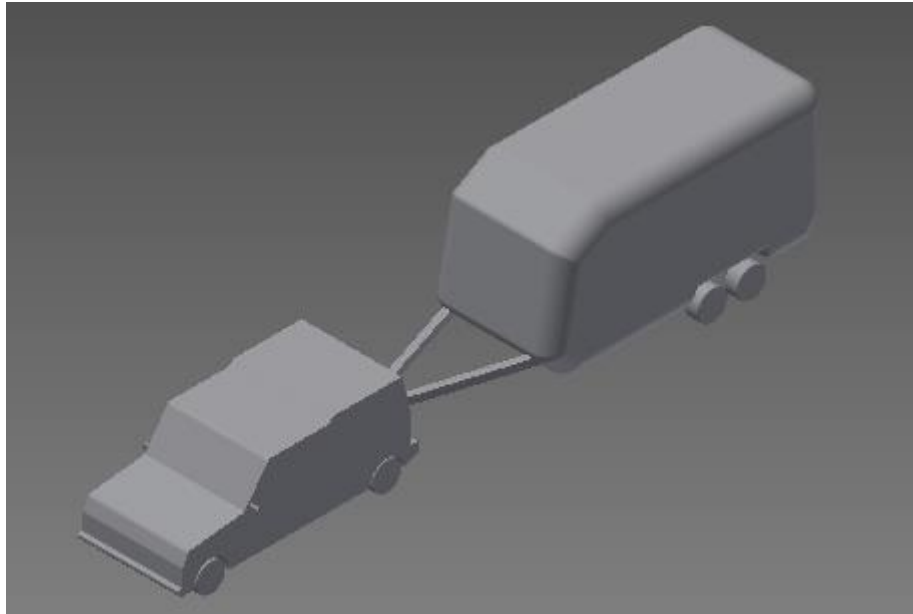
Figure 5.2: 350mm Caravan Edge Radius

5.1.3 Caravan Frontal Vanes

From the pre-optimization study it was noted that the airflow between the tow vehicle and the caravan was turbulent. As the caravan was rotated into the flow the air flowed a path around the lower front edges of the caravan and the turbulent eddies circulated down the leeward side of the caravan.

From the literature review conducted it was noted placing a barrier like device across the front face of the trailer would aid to trap this air and encourage vortices to form which would re energise the air and aid it in travelling up over the caravan.

The vanes follow a similar approach to wing fences on aircraft and are deemed effective for reducing flow in the lateral direction. The vanes were created by extruding four rectangular plates of dimension 1380 mm by 280 mm. These plates were then given 40 mm radius rounding to the leading edge. The plates were positioned 450 mm apart.

The caravan design that offered the greatest improvement to its aerodynamics would be fitted with the vane system and a further analysis would be conducted to validate its inclusion.
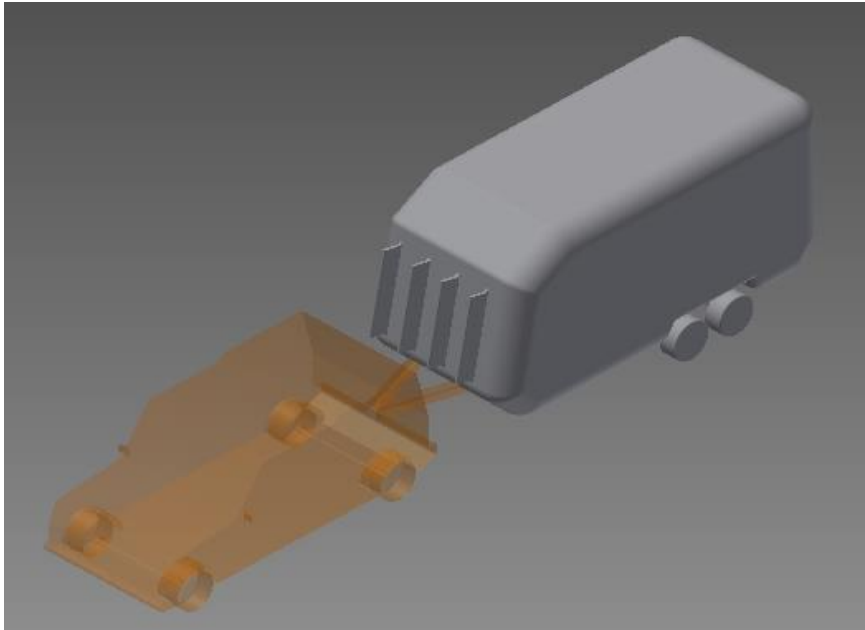
Figure 5.3: Caravan Frontal Vane Modification

CHAPTER 6 – RESULTS & DISCUSSION

6.1 Overview

This chapter contains the results obtained through carrying out a parametric study on the baseline caravan. It details the results of five different configurations and compares them to the original baseline caravan configuration with 1.8m draw bar. Listed within this section are also results of calculations for specific coefficients of force using data derived from the simulations as listed in Appendices E through N. These tables contain important data such as;

- Configuration of caravan
- Wind velocity
- Forces in x, y & z
- Modification Detail
- Mesh Statistics
- Iterations to Convergence

6.2 Crosswind Coefficient Calculations

Utilising the equations in Section 2.12 the following coefficients were obtained as summarised in the following tables.

Table 14: Drag Coefficient for 1.8m Draw Bar

Caravan Drawbar (m)	Velocity (m/s)	Wind Angle	Force_x (N)	Cd
1.8	13.89	0	560.3	0.70
1.8	22.22	0	1436.1	0.70
1.8	27.78	0	2244.4	0.70
1.8	13.89	15	876.8	0.50
1.8	22.22	15	2244.7	0.50
1.8	27.78	15	3507.6	0.50
1.8	13.89	30	1434.8	0.55
1.8	22.22	30	3674.6	0.55
1.8	27.78	30	5742.9	0.55
1.8	13.89	45	2040.4	0.62
1.8	22.22	45	5226.4	0.62
1.8	27.78	45	8168.2	0.62
1.8	13.89	60	2492.1	0.67
1.8	22.22	60	6383.9	0.67
1.8	27.78	60	9977.7	0.67

Table 15: Drag Coefficients for 1.5m Draw Bar

Caravan Drawbar (m)	Velocity (m/s)	Wind Angle	Force_x (N)	Cd
1.5	13.89	0	555.8	0.70
1.5	22.22	0	1420.9	0.70
1.5	27.78	0	2220.7	0.70
1.5	13.89	15	854.3	0.48
1.5	22.22	15	2186.5	0.48
1.5	27.78	15	3416	0.48
1.5	13.89	30	1401.5	0.53
1.5	22.22	30	3588.6	0.53
1.5	27.78	30	5607.7	0.53
1.5	13.89	45	1994.7	0.61
1.5	22.22	45	5108	0.61
1.5	27.78	45	7983.4	0.61
1.5	13.89	60	2421	0.65
1.5	22.22	60	6203.2	0.65
1.5	27.78	60	9696.5	0.65

Table 16: Drag Coefficients for 1.0m Draw Bar

Caravan Drawbar (m)	Velocity (m/s)	Wind Angle	Force_x (N)	Cd
1.0	13.89	0	517.2	0.65
1.0	22.22	0	1324	0.65
1.0	27.78	0	2068.9	0.65
1.0	13.89	15	850.1	0.48
1.0	22.22	15	2176.4	0.48
1.0	27.78	15	3400.6	0.48
1.0	13.89	30	1350.3	0.51
1.0	22.22	30	3458.1	0.52
1.0	27.78	30	5404.3	0.52
1.0	13.89	45	1904	0.58
1.0	22.22	45	4876.4	0.58
1.0	27.78	45	7620.7	0.58
1.0	13.89	60	2359.2	0.63
1.0	22.22	60	6043.6	0.63
1.0	27.78	60	9445.7	0.63
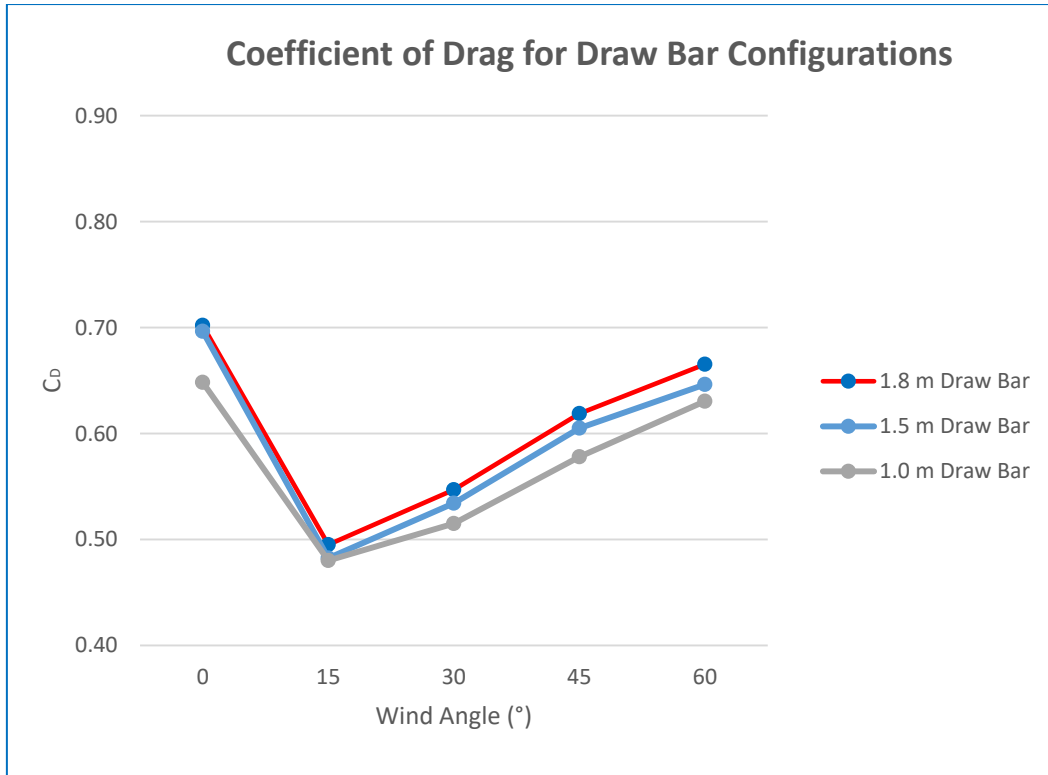
Figure 6.1: Drag Coefficients for Modified Caravan Draw Bar

Table 17: Lift Coefficient for 1.8m Draw Bar

Caravan Drawbar (m)	Velocity (m/s)	Wind Angle	Force_y (N)	C_L
1.8	13.89	0	83.8	0.11
1.8	22.22	0	217.5	0.11
1.8	27.78	0	340.6	0.11
1.8	13.89	15	61.7	0.03
1.8	22.22	15	153.2	0.03
1.8	27.78	15	236.1	0.03
1.8	13.89	30	241.2	0.09
1.8	22.22	30	611.4	0.09
1.8	27.78	30	951.4	0.09
1.8	13.89	45	297.3	0.09
1.8	22.22	45	756.5	0.09
1.8	27.78	45	1178.8	0.09
1.8	13.89	60	387.3	0.10
1.8	22.22	60	980.6	0.10
1.8	27.78	60	1524.8	0.10

Table 18: Lift Coefficient for 1.5m Draw Bar

Caravan Drawbar (m)	Velocity (m/s)	Wind Angle	Force_y (N)	C_L
1.5	13.89	0	80.4	0.10
1.5	22.22	0	206.9	0.10
1.5	27.78	0	324.37	0.10
1.5	13.89	15	120.5	0.07
1.5	22.22	15	305.5	0.07
1.5	27.78	15	475.2	0.07
1.5	13.89	30	209.8	0.08
1.5	22.22	30	533.4	0.08
1.5	27.78	30	830.9	0.08
1.5	13.89	45	360.8	0.11
1.5	22.22	45	921.9	0.11
1.5	27.78	45	1439	0.11
1.5	13.89	60	468.2	0.12
1.5	22.22	60	1196.2	0.12
1.5	27.78	60	1865.6	0.12

Table 19: Lift Coefficient for 1.0m Draw Bar

Caravan Drawbar (m)	Velocity (m/s)	Wind Angle	Force_y (N)	C_L
1.0	13.89	0	60	0.08
1.0	22.22	0	153.4	0.08
1.0	27.78	0	241.4	0.08
1.0	13.89	15	72.9	0.04
1.0	22.22	15	183.8	0.04
1.0	27.78	15	285.1	0.04
1.0	13.89	30	150.6	0.06
1.0	22.22	30	382.9	0.06
1.0	27.78	30	596.5	0.06
1.0	13.89	45	244.8	0.07
1.0	22.22	45	621.7	0.07
1.0	27.78	45	968	0.07
1.0	13.89	60	431.7	0.12
1.0	22.22	60	1097.9	0.11
1.0	27.78	60	1710.2	0.11

Coefficient of Lift for Draw Bar Configurations
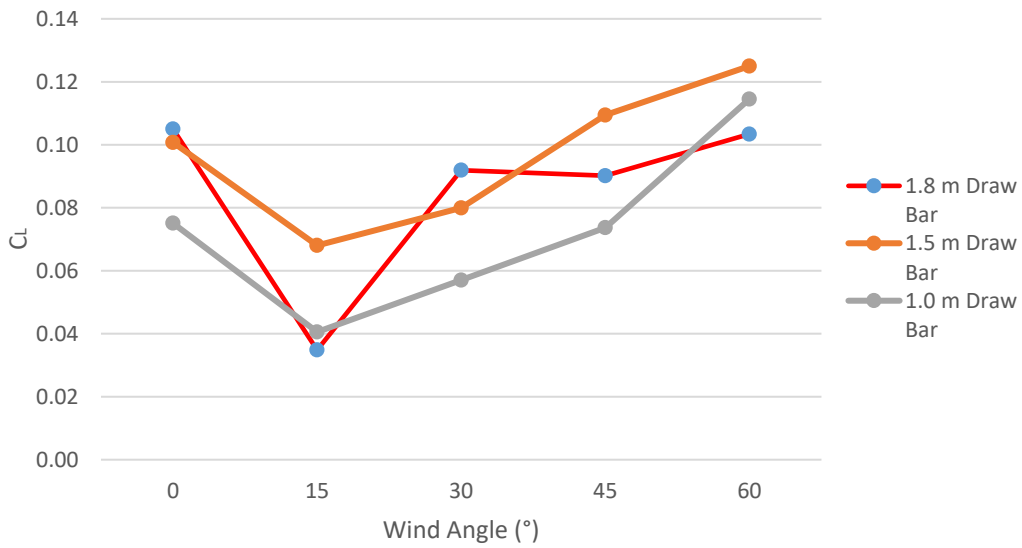
Figure 6.2: Lift Coefficients for Modified Caravan Draw Bar

Table 20: Side Force Coefficient for 1.8 m Draw Bar

Caravan Drawbar (m)	Velocity (m/s)	Wind Angle	Force_z (N)	C_S
1.8	13.89	0	20	0.03
1.8	22.22	0	56.6	0.03
1.8	27.78	0	89.1	0.03
1.8	13.89	15	628.8	0.36
1.8	22.22	15	1613	0.36
1.8	27.78	15	2522.9	0.36
1.8	13.89	30	1167.5	0.45
1.8	22.22	30	2989.1	0.45
1.8	27.78	30	4673.2	0.45
1.8	13.89	45	1247.3	0.38
1.8	22.22	45	3197.8	0.38
1.8	27.78	45	4999.9	0.38
1.8	13.89	60	1080.6	0.29
1.8	22.22	60	2769.2	0.29
1.8	27.78	60	4328.6	0.29

Table 21: Side Force Coefficients for 1.5m Draw Bar

Caravan Drawbar (m)	Velocity (m/s)	Wind Angle	Force_z (N)	Cs
1.5	13.89	0	12.1	0.02
1.5	22.22	0	30.7	0.02
1.5	27.78	0	48	0.02
1.5	13.89	15	636.2	0.36
1.5	22.22	15	1631.3	0.36
1.5	27.78	15	2550.6	0.36
1.5	13.89	30	1147	0.44
1.5	22.22	30	2940.2	0.44
1.5	27.78	30	4596.7	0.44
1.5	13.89	45	1307.6	0.40
1.5	22.22	45	3352.7	0.40
1.5	27.78	45	5241.9	0.40
1.5	13.89	60	1128.2	0.30
1.5	22.22	60	2894.2	0.30
1.5	27.78	60	4526.2	0.30

Table 22: Side Force Coefficients for 1.0m Draw Bar

| Caravan Drawbar (m)	Velocity (m/s)	Wind Angle	Force_z (N)	Cs
1.0	13.89	0	11.1	0.01
1.0	22.22	0	28.5	0.01
1.0	27.78	0	44.6	0.01
1.0	13.89	15	617.5	0.35
1.0	22.22	15	1584.9	0.35
1.0	27.78	15	2479.1	0.35
1.0	13.89	30	1082.6	0.41
1.0	22.22	30	2776.9	0.41
1.0	27.78	30	4342.6	0.41
1.0	13.89	45	1234.6	0.37
1.0	22.22	45	3163.4	0.37
1.0	27.78	45	4944.5	0.37
1.0	13.89	60	1096.9	0.29
1.0	22.22	60	2811.4	0.29
1.0	27.78	60	4395.2	0.29
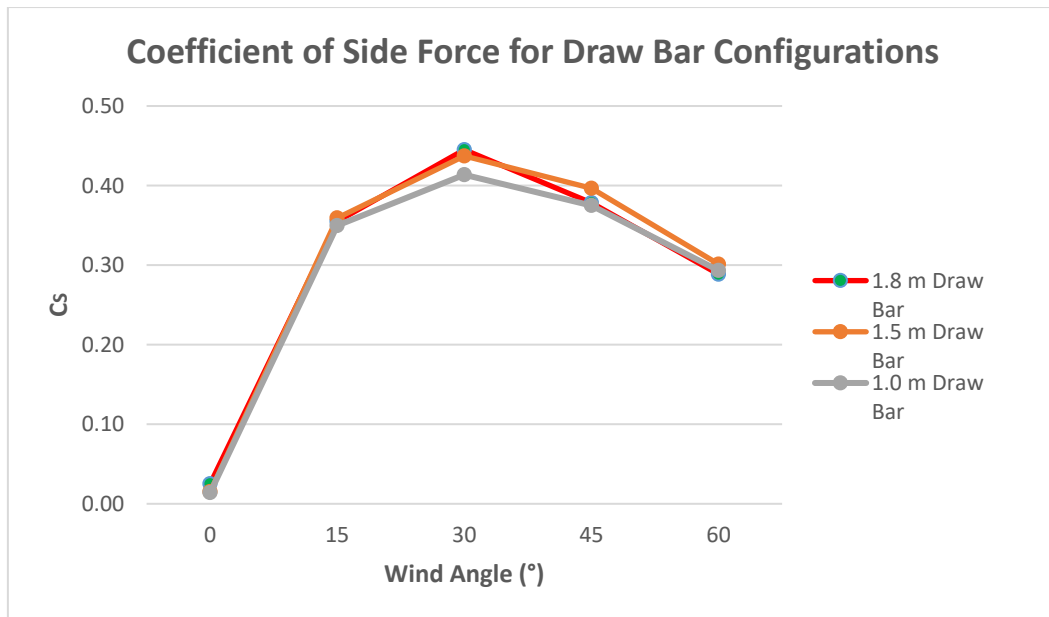
Figure 6.3: Side Force Coefficients for Modified Caravan Draw Bar

6.3 Geometry Variation

This section discusses the impact that each geometry variation has on the aerodynamic efficiency of the caravan.

6.3.1 Draw Bar Modification

It is observed through the simulations at a wind speed of 80 km/hr that as the draw bar is reduced in length the Force in the x direction reduces. The difference between the baseline length and the 1.0 m Draw bar is 340 N.

When looking at the forces in the y direction it is observed that the 1.0 m draw bar demonstrates the greatest reduction in lift forces especially at angle between 30° and 45°.

The 1.0 m Draw bar shows it is the better of the options for minimising the side forces in the z direction. This is amplified at wind angles above 30°.

The full results for the Draw Bar Analysis can be located in Appendix E, F and G.
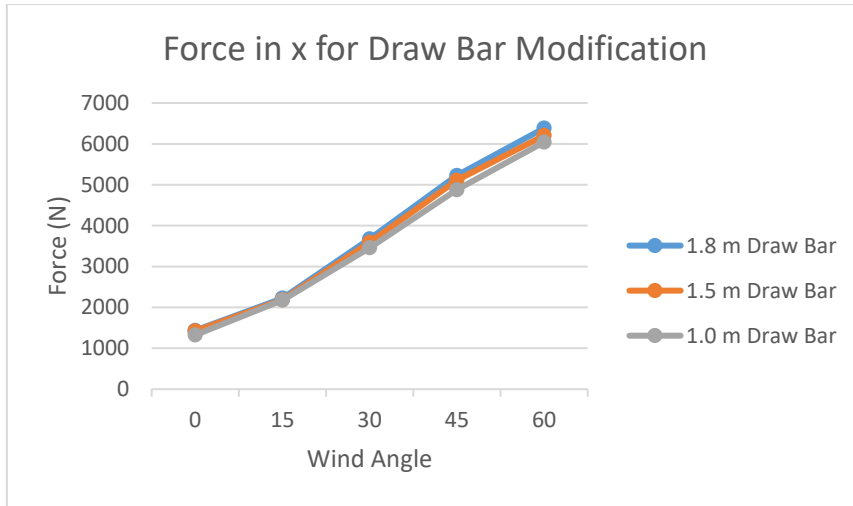
Figure 6.4: Draw Bar Forces in x Direction
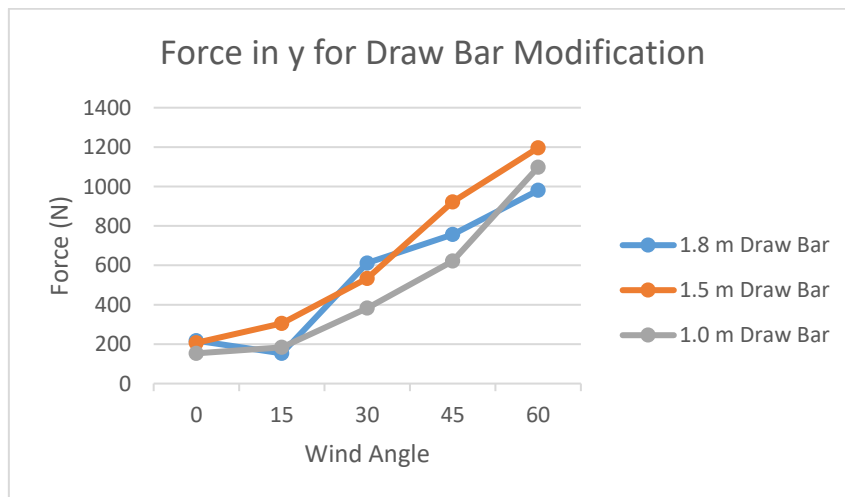
Figure 6.5: Draw Bar Forces in y Direction
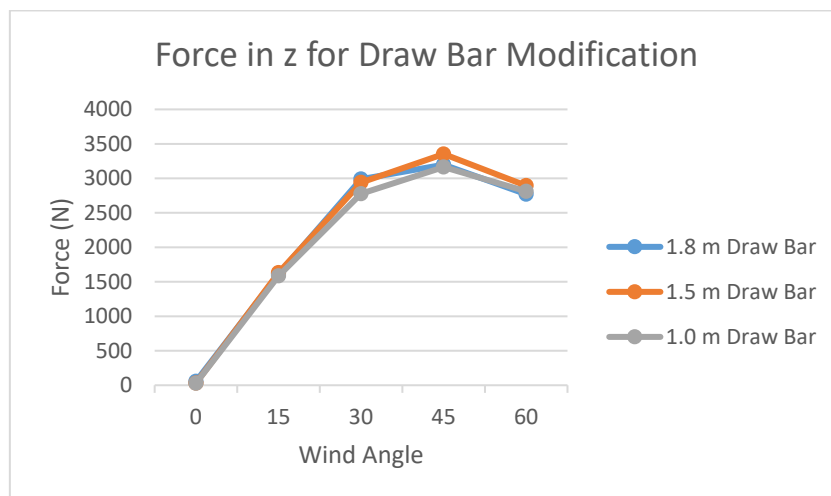
Figure 6.6: Draw Bar Forces in z Direction
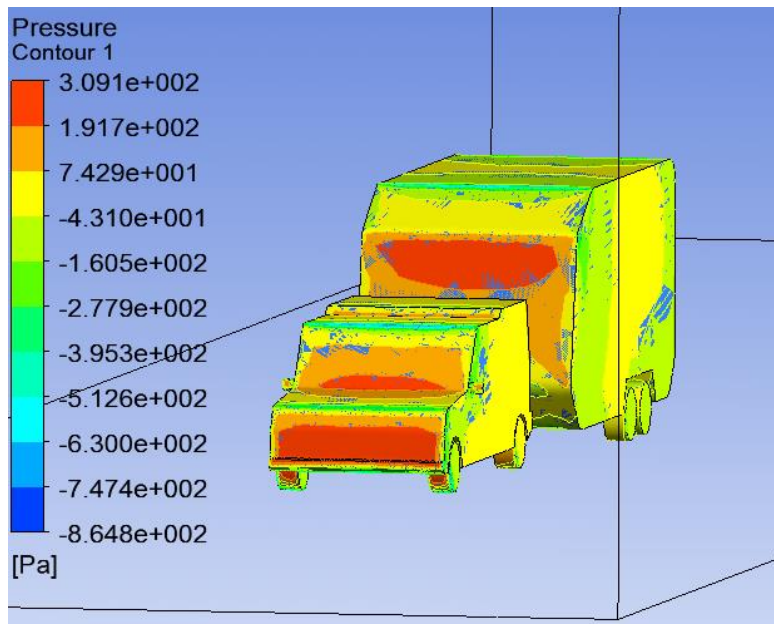
Figure 6.7: Pressure Distribution on Caravan with 1.0 m Draw Bar

It was observed that as the draw bar was reduced in length, the area on the front of the caravan that shows the higher pressure distribution shifts vertically. This is due to the reducing gap between the car and the caravan. The airflow as it leaves the roof of the tow vehicle strikes higher up the front of the caravan, this reducing the size of the high pressure contact patch.

6.3.2 Edge Radius Modification

The edge radius modification results show a significant improvement in the streamlining of the caravan body profile. This initial baseline caravan produced a force in the x direction of 1436.1 N with an airflow velocity of 80 km/hr and the caravan position directly into the flow. With the addition of a 100 mm edge radius the force is observed to reduce to 1265.6 N which is a reduction of 170.5 N.

Using the fuel consumption calculation method in Chapter 3, based on proportionality to the stipulated Land Rover economy figures, this equates to a reduction of 2.6 l/100 km.
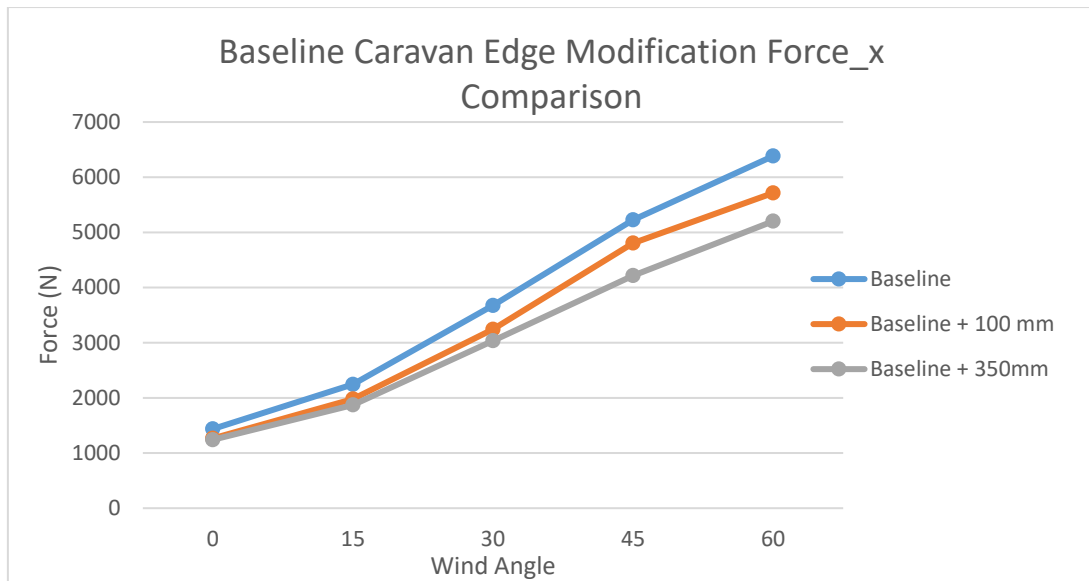
Figure 6.8: Baseline Caravan Edge Modification Comparison

It is observed that the 350 mm edge radius provides the largest reduction in force figures under all wind direction configurations. Utilising the 350 mm edge radius on the baseline caravan provides a 195 N reduction in force.

The rounded edges also serve to provide a smoother transition for the airflow travelling around the edge. It can be seen from the streamline plot that the air flows past the front and rear edge of the caravan and stays closer to the surface.
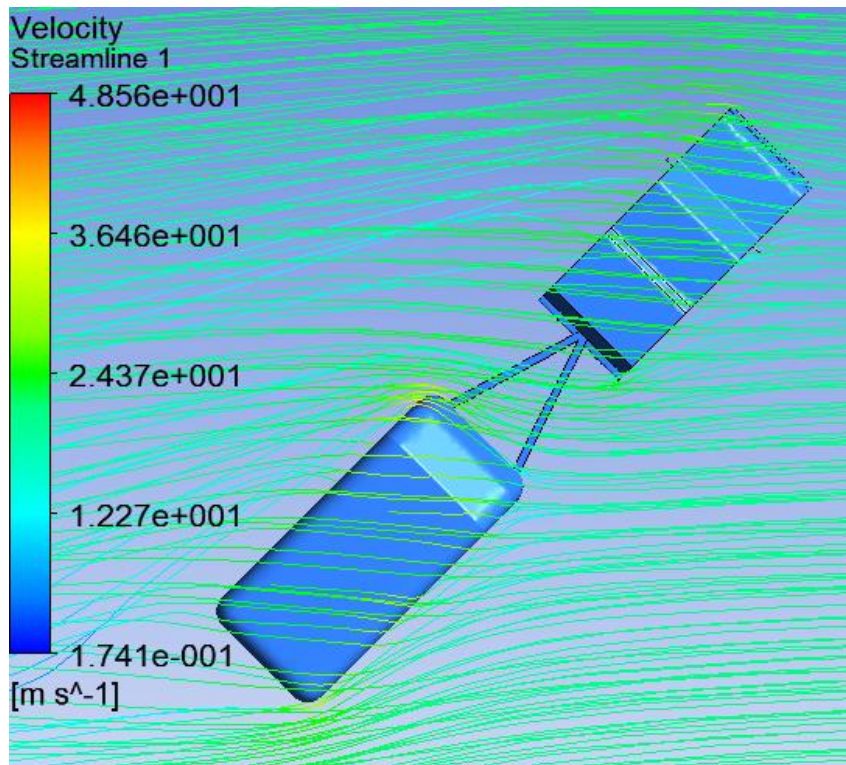
Figure 6.9: 350mm Edge at 45° flow

6.3.3 Frontal Vane Modification

The final modification analysed was the inclusion of a vane type assembly to the front of the caravan. The results demonstrate an even further reduction in force in the x direction. The final caravan model featuring the 1.0m draw bar with 350mm rounded edges with the addition of the vane assembly, was simulated under initial conditions of 80 km/hr air flow at 0° Yaw. The results show a force of 1170 N which is a reduction of 266 N over the initial baseline caravan.

The streamline plot show in addition to the airflow conforming to the rounded edges, part of the airflow becomes trapped between the outer vanes and a rotational flow is created as it makes its way up the front surface of the caravan and spills over the roof.
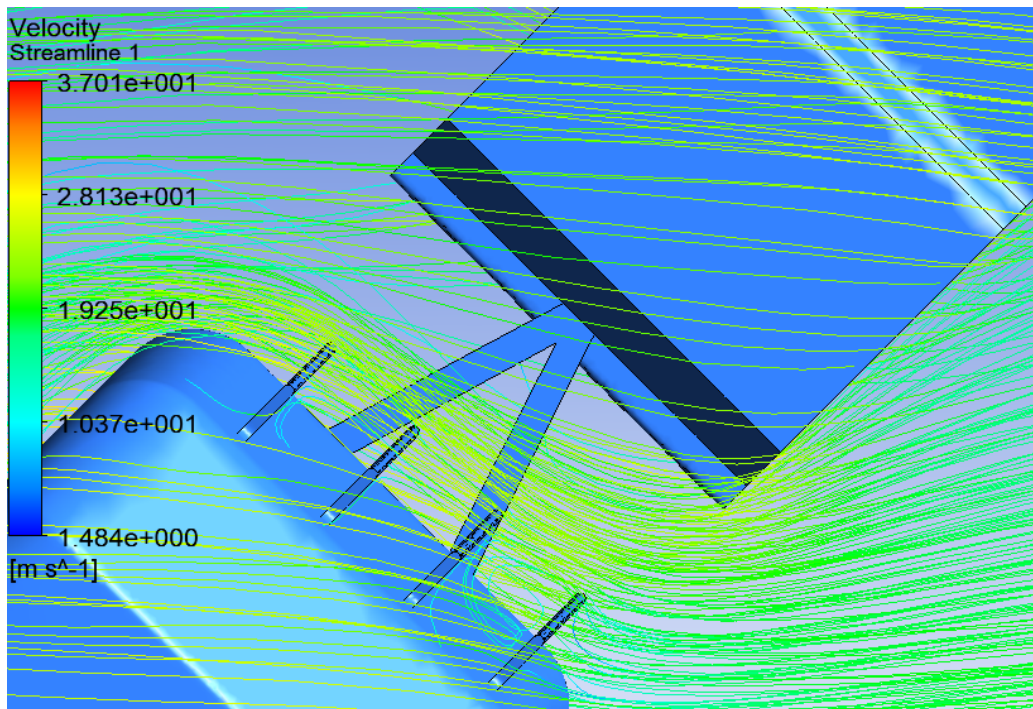
Figure 6.10: Velocity Streamlines of Final Caravan Design

6.4 Fuel Efficiency Calculations

Based on the reduction of 266 N in the x direction over the baseline configuration, the following estimate can be made regarding the theoretical improvement in fuel economy of the tow vehicle. Given that the calculations are based on proportionality to the established data and not based on engine power curves and other specific details regarding the tow vehicle, it is recommended that a more detailed assessment be made regarding other contributing factors.

Original Force for Baseline Caravan: 1436.1 N

Optimised Caravan (1.0 m Draw Bar, 350 mm Edge & Frontal Vane): 1170.4 N

Landrover Force_x: 568 N

Original Calculated Fuel Economy of Tow Vehicle with Baseline Caravan: 22.2 l/100 km

Therefore: $\frac{1170.4}{568} \times 8.8 = 18.1 \ L/100km$

Reduction of 4.1 l/100km

CHAPTER 7 - CONCLUSION

7.1 Overview

This final chapter discusses the findings of this study and presents some guiding recommendations to the implementation of the modifications explored during the optimisation study. It also introduces future work to consider in order to validate these results. Detailed within are also limitations encountered during the study and recommendations on how to possibly address them.

7.2 Conclusions

In line with Project Specification, this study progressed through various important stages resulting in the final results being obtained, regarding the improvement of the caravan design by modelling crosswind flow. The important first stage was to understand the problem statement as provided by the Engineering Faculty at USQ. Once understood the project moved into undertaking a literature review regarding crosswind flow effects on vehicles. It was noted very early on that there was limited literature on optimising caravan designs that focussed on crosswind effects. Reviewing the effects of crosswinds on other transportation methods allowed for parallel to be drawn that would be relevant to the tow vehicle caravan scenario. The importance of understanding CFD methods was critical to the undertaking of this project.

Following the literature models of the tow vehicle and caravan were produced for use in the CFD simulation. The initial study conducted on the baseline caravan allowed for some important data to be collected which would later be used to compare against the modified results. The parametric study focused carrying out modifications to the caravan in order to validate their effectiveness through CFD.

The results obtained showed that there was scope to improve the caravan's aerodynamic properties by up to 18% which preliminary calculations indicate could enhance the tow vehicles fuel economy whilst towing by approximately 4 litres per hundred kilometres of driving.

These results are promising keeping in mind that further work would need to be carried out to assess the practicality of the final design.

7.3 Limitations and Future Work

Two limitations identified during the early stages of this study involve the modelling of tow vehicle and caravan and the meshing used in the CFD simulations. The three dimensional models created could have been created with greater accuracy however it was decided that due to high computing requirements in meshing the models were simplified. It is expected that the models would produce less accurate results however it was decided that this would be acceptable for this study.

The meshing quality was also experimented with and was subsequently reduced in order to manage the time available for simulation. It would be possible using a high end computer processor to handle these computations efficiently with an expected increase in accuracy.

As detailed in the Project Specification there is scope for performing the simulations using transient wind loading as would be expected in normal every day driving.

In order to validate the results obtained through the CFD analysis it would be expected that scale models would be produced and tested in a wind tunnel, to obtain force figures for comparison. The wind tunnel could also be used to perform particle image velocimetry in order to capture the flow lines around the model.

In addition the expansion of this study to carry out an analysis of the dynamic response of the caravan to the wind would be beneficial in order to assess vehicle handling and safety issues.

LIST OF REFERENCES

Aerodynamics, 2011 Swift Group Caravans, United Kingdom, viewed 18 March 2016, <swiftrv.com.au/wp-content/uploads/2013/01/CFD_study.pdf>

Asress, MB & Svorcan, J 2014, 'Numerical investigation on the aerodynamic characteristics of high-speed train under turbulent crosswind', Journal of Modern Transportation, vol. 22, no. 4, pp. 225-234, http://dx.doi.org/10.1007/s40534-014-0058-7

Bakker, A, 2002, 'Applied Computational Fluid Dynamics', Lecture 7 Meshing, viewed 14 June 2016, www.bakker.org

Basson, J 2013, 'Analysis of the aerodynamic attributes of motor vehicles', B.Eng thesis, University of Southern Queensland, Toowoomba.

Briskey, K 2013, 'Improving Caravan Design by Modelling of Airflow', B.Eng thesis, University of Southern Queensland, Toowoomba.

Cambridge Dictionary, 2016, Crosswind, Cambridge University Press, viewed 08 May 2016, <http://dictionary.cambridge.org/dictionary/english/crosswind>

Carfolio, 2013, LandRover Discovery Specifications, viewed 03 May 2016, <http://www.carfolio.com/specifications/models/?man=6801>

Engineers Australia 2016, Western Australia Division, Engineers Australia–Code of Ethics, viewed 13 May 2016, <https://www.engineersaustralia.org.au/western-australia-division/code-ethics>

ERP 2016, Project Specification, Improving Caravan Design by Modelling of Airflow, University of Southern Queensland, viewed 5 March 2016, <http://usqstudydesk.usq.edu.au/m2/pluginfile.php/641537/mod_resource/content/2/V2/ProjectListAll-auto.html>

Feasibility Study into the Aerodynamic Improvement of Caravans, Gleyndwr University, Wales, viewed 12 March 2016, http://www.astutewales.com/en/getfile.php?type=site_documents&id=31.%20Case%20Study%20Fifth%20Wheel%20(updated%2019_06_2014).pdf

Frei, W, 2013, Comsol Blog, 'Introduction to Turbulence Modelling', viewed 18 July 2016, https://www.comsol.com/blogs/which-turbulence-model-should-choose-cfd-

High Speed Rail History, 2015, UIC, France, viewed 04 May 2016, <http://www.uic.org/High-Speed-History>

Hillocks, M 2015, 'Design of a Low Drag Caravan',B.Eng thesis, University of Southern Queensland, Toowoomba.

Johnson, FT, Tinoco, EN & Yu, NJ 2005, 'Thirty years of development and application of CFD at Boeing Commercial Airplanes, Seattle', Computers & Fluids, vol. 34, no. 10, pp. 1115-1151, <http://www.sciencedirect.com/science/article/pii/S0045793005000125>

Johnston, D,U.S Centennial of Flight Commission , Early Developments in Aerodynamics, viewed 10 May 2016, http://www.centennialofflight.net/essay/Theories_of_Flight/early_aero/TH3.htm

Keating, M, 2010 , Strategies to Achieve Reliable and Accurate CFD Solutions, ANSYS UK.

Kee, JD, Rho, JH, Kim, KH & Lee, DH 2014, 'High speed driving stability of passenger car under crosswind effects', International Journal of Automotive Technology, vol. 15, no. 5, pp. 741-747, http://dx.doi.org/10.1007/s12239-014-0077-8

Kuron, M , 2015, 3 Criteria for assessing CFD Convergence, viewed 12 June 2016, http://www.engineering.com/DesignSoftware/DesignSoftwareArticles/ArticleID/9296/3-Criteria-for-Assessing-CFD-Convergence.aspx

Kuzmin, D, 2012, Lecture Notes – Introduction to Computational Fluid Dynamics, University of Dortmund, accessed 12 June 2016, http://www.mathematik.uni-dortmund.de/~kuzmin/cfdintro/lecture1.pdf

Discovery 4 Specification Sheet, Land Rover 2016, http://www.landrover.com.au/vehicles/discovery4/index.html

Malviya, V , Gundala, M and Mishra, R, 2009, Effect of Crosswind on Aerodynamic Coefficients of Ground Vehicles, University of Huddersfield ,pp. 19-20.

Mansor, S., Rahman, M.R. and Passmore, M.A., Dynamic Simulation of Vehicle Crosswind Sensitivity for Various Rear Slant Angle.

Mass Production of Cars, 2016, Dorling Kindersley Limited, England, viewed 03 June 2016, http://www.dkfindout.com/uk/transport/history-cars/mass-production/

NTI's Guide to the Trucking Industry, National Transport Insurance, 2011, viewed 17 August 2016, https://www.nti.com.au/intermediaries/insurance/ntis-guide-to-the-trucking-industry-2016.php

Pritchard, PJ 2011, Fox and McDonald's Introduction to Fluid Mechanics, 8th edn. John Wiley & Sons, p.207.

Suzuki, M, Tanemoto, K & Maeda, T 2003, 'Aerodynamic characteristics of train/vehicles under cross winds', Journal of Wind Engineering and Industrial Aerodynamics, vol. 91, no. 1–2, pp. 209-218, http://www.sciencedirect.com/science/article/pii/S016761050200346X

USQ 2016, ENG4111 Research Project Part 1 Project Reference Book, University of Southern Queensland, Toowoomba.

APPENDICES

Appendix A - Project Specification

University of Southern Queensland

FACULTY OF ENGINEERING AND SURVEYING

ENG 4111/4112 Research Project

PROJECT SPECIFICATION

For:	Adrian De Leon
Title:	Improving Caravan Design by Modelling of Crosswind
Major:	Mechanical Engineering
Supervisors:	Dr. Andrew Wandel
Enrolment:	ENG4111 – EXT S1, 2016 ENG4112 – EXT S2, 2016
Project Aim:	This project seeks to investigate the efficiency gains from improvements made to caravan design subject to crosswind airflow, through the implementation of a Computational Fluid Dynamic (CFD) analysis.

Programme: **Issue A, 16th March 2016**

1. Research background information related to caravan drag profiles and towing vehicle performance through CFD modelling.

2. Research geometry and performance data for subject caravan and tow vehicle.

3. Create 3D model of Caravan and Tow Vehicle for use in CFD analysis.

4. Validate 3D model using a headwind analysis.

5. Undertake CFD simulation of current prototype under cross wind conditions.

6. Investigate/Propose performance enhancing modifications to initial baseline design.

7. Perform CFD analysis and parametric study on modified caravan.

If time permits:

8. Propose further modifications.

9. Investigate dynamic stability of caravan and tow vehicle combination subject to cross wind.

Perform transient simulation of caravan/tow vehicle movement due to cross wind loading.

Appendix B - Project Timelines

Project Timeline
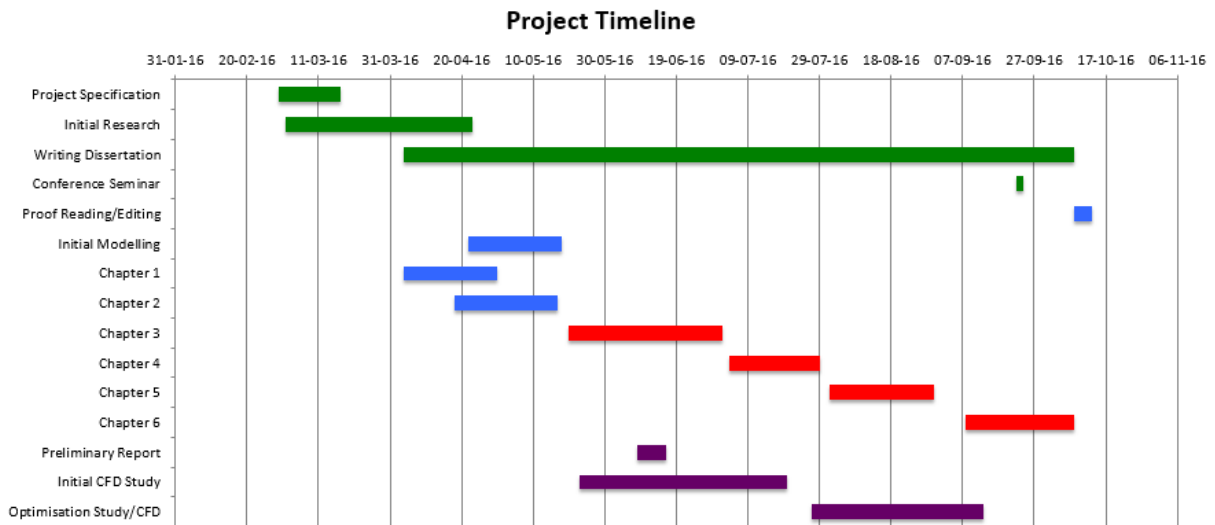
Task Name	Start	End	Duration (days)
Project Specification	29-02-16	16-03-16	17
Initial Research	02-03-16	22-04-16	52
Writing Dissertation	04-04-16	07-10-16	187
Conference Seminar	22-09-16	23-09-16	2
Proof Reading/Editing	08-10-16	12-10-16	5
Initial Modelling	22-04-16	17-05-16	26
Chapter 1	04-04-16	29-04-16	26
Chapter 2	18-04-16	16-05-16	29
Chapter 3	20-05-16	01-07-16	43
Chapter 4	04-07-16	29-07-16	25
Chapter 5	01-08-16	29-08-16	29
Chapter 6	08-09-16	07-10-16	30
Preliminary Report	08-06-16	15-06-16	8
Initial CFD Study	23-05-16	19-07-16	58
Optimisation Study/CFD	27-07-16	12-09-16	48

Project Milestones

Project Progress Assessment – 15 June 2016

Partial Draft Dissertation – 07 September 2016

Dissertation Submission – 13 Oct 2016

Appendix C - Risk Assessment

Risk mitigation over certain phases of this research is performed by assessing both the likelihood and consequence of the potential danger in order to make an assessment of the hazards presented and decide how to proceed.

Likelihood

Defined as the probability of an event occurring that will lead to a particular consequence.

Likelihood can be categorised into the following five categories in order of likelihood;

1. Rare
2. Unlikely
3. Possible
4. Likely
5. Almost Certain

Likelihood	Description	Frequency
Almost certain	Expected to occur in most circumstances	Likely to occur more than once per year
Likely	Probably occur in most circumstances	Likely to occur approximately once per year
Possible	Could occur at sometime	Likely to occur approximately once every five years
Unlikely	Not expected to occur	Likely to occur approximately once every five to ten years
Rare	Exceptional circumstances only	Likely to occur with less frequency than once every ten years

Table 23: Likelihood Category Table

Consequence

Defined as the outcome of the hazardous event. It is based on the direct effect to the individual or group.

Consequence is categorised into the following five categories in order of consequence;

1. Negligible

2.   Minor

3.   Moderate

4.   Major

5.   Severe

Rating	Consequence
Severe	Death or multiple life threatening injuries.
Major	Life threatening injury or multiple serious injuries causing hospitalisation.
Moderate	Serious injury causing hospitalisation.
Minor	Minor injury requiring medical treatment and / or lost time from the workplace.
Negligible	Ailments requiring first aid treatment - minor cuts, bruises, bumps.

Table 24: Consequence Category Table

Both Likelihood and Consequence are used as inputs into a Risk Matrix which is used to determine the level of risk and subsequently treat the risk as appropriate.

Likelihood	Consequence				
	Negligible	Minor	Moderate	Major	Severe
Almost certain	Low	Medium	High	Very High	Very High
Likely	Low	Medium	High	High	Very High
Possible	Low	Medium	Medium	High	High
Unlikely	Low	Low	Medium	Medium	High
Rare	Low	Low	Low	Medium	Medium

Table 25: Risk Management Matrix (Australian Sports Commission)

The following two hazards were identified as being relevant to this research project. They have been analysed through the Risk Management Matrix and Risk mitigation strategies developed.

Hazard 1 – Extended Computer Use/ Incorrect Workstation Ergonomic Setup

Likelihood Level	Almost Certain
Consequence Level	Minor
Risk Level	Medium
Mitigation Strategy	1. Ensure routine breaks away from workstation are taken 2. Ensure lighting is adequate in room 3. Adjust Monitor Display Properties 4. Ensure correct sitting posture is maintained 5. Exercise eyes 6. Blink more often than usual
Treated Risk Level	Low – Deemed an acceptable level of risk to carry

Table 26: Hazard 1 Risk Assessment

Hazard 2 – Car Accident during travel to Residential School for Project Conference

Likelihood Level	Possible
Consequence Level	Severe
Risk Level	High
Mitigation Strategy	1. Take frequent breaks from driving 2. Drive according to the road conditions 3. Plan route carefully 4. Ensure vehicle is roadworthy 5. Ensure communication strategy in place in the event of complications
Treated Risk Level	Medium – This is still an unacceptable level of risk which requires further mitigation

Table 27: Hazard 2 Risk Assessment

Appendix D – Land Rover Specifications

Overall length 4,829mm

Front wheel track 1,605mm

Rear wheel track 1,612.5mm

Width 2,053mm mirrors folded
Width 2,200mm mirrors out

Obstacle Clearance
Off-road height up to 310mm
Standard ride height up to 185mm
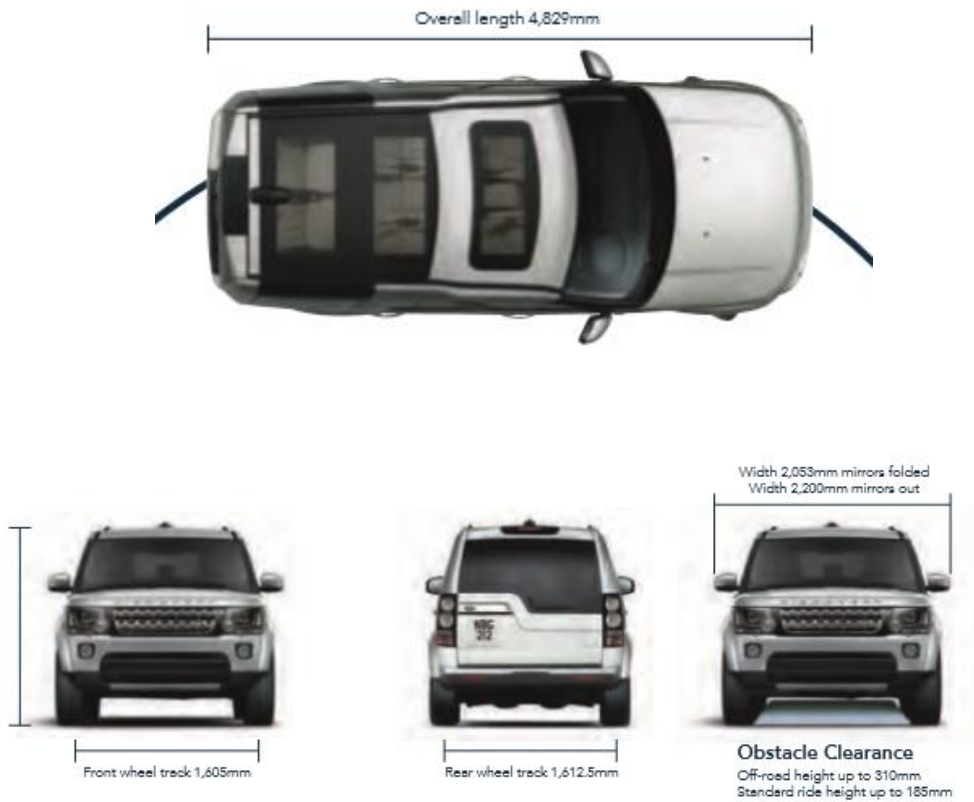
Standard Ride Height
With Alpine glass roof (not open): 1,882mm
With fixed roof: 1,887mm
With roof rails: 1,891mm
With Alpine glass roof (open): 1,920mm
With DAB radio antennae: 1,938mm
With roof rails and crossbar fitted: 1,980mm
Access height setting, only available with air
suspension, will reduce each of the above by 50mm

Loadspace Capacity
Rear seats upright
Height 1,027mm (1,058mm with Alpine roof),
Width 1,235mm
Loadspace volume 1,260 litres
Loadspace width between arches 1,146mm
Rear seats folded
Height 1,027mm (1,058mm with Alpine roof),
Width 1,235mm
Loadspace volume 2,558 litres
Loadspace width between arches 1,146mm
Maximum length at floor 1,950mm

Ride Height	A Approach Angle	B Ramp Angle	C Departure Angle
Off-road	36.2°	27.3°	29.6°
Standard	32.2°	22.8°	26.7°

Appendix E – Baseline Caravan Data Sheet (1.8 m Draw Bar)

Table 28: Caravan 1.8m Draw Bar Data

DrawBar Length (m)	Wind Velocity (m/s)	Speed (km/h)	Wind Angle	Nodes	Elements	Force x (N)	Force y (N)	Force z (N)	Convergence Iterations
1.8	13.8	50	0	119876	575961	560.3	80.2	19.5	138
1.8	22.22	80	0	119876	575961	1436.1	217.5	56.6	107
1.8	27.77	100	0	119786	575961	2244.4	340.6	89.1	106
1.8	13.8	50	15	119369	573889	876.8	61.7	628.4	87
1.8	22.22	80	15	119369	573889	2244.7	153.2	1613	86
1.8	27.77	100	15	119369	573889	3507.6	236.1	2522.9	86
1.8	13.8	50	30	119688	574918	1434.8	241.2	1166	62
1.8	22.22	80	30	119688	574918	3674.6	611.4	2989.1	64
1.8	27.77	100	30	119688	574918	5742.9	951.4	4673.2	65
1.8	13.8	50	45	110873	537001	2040.4	297.3	1247.3	78
1.8	22.22	80	45	110873	537001	5226.4	756.5	3197.8	78
1.8	27.77	100	45	110873	537001	8168.2	1178.8	4999.9	78
1.8	13.8	50	60	116295	562929	2492.1	387.3	1080.6	75
1.8	22.22	80	60	116295	562929	6383.9	980.6	2769.2	75
1.8	27.77	100	60	116295	562929	9977.7	1524.8	4328.6	75

Appendix F - Caravan 1.5 m Draw Bar Data Sheet

Table 29: Caravan 1.5m Draw Bar Data

DrawBar Length (m)	Wind Velocity (m/s)	Speed (km/h)	Wind Angle	Nodes	Elements	Force x (N)	Force y (N)	Force z (N)	Iter
1.5	13.8	50	0	120028	576721	555.8	80.4	12.1	94
1.5	22.22	80	0	120028	576721	1420.9	206.9	30.4	95
1.5	27.77	100	0	120028	576721	2220.7	324.4	48	100
1.5	13.8	50	15	115175	557118	854.3	120.5	636.2	79
1.5	22.22	80	15	115175	557118	2186.5	305.5	1631.3	79
1.5	27.77	100	15	115175	557118	3416	475.2	2550.6	79
1.5	13.8	50	30	115055	555670	1401.5	209.8	1147	61
1.5	22.22	80	30	115055	555670	3588.6	533.4	2940.2	61
1.5	27.77	100	30	115055	555670	5607.7	830.9	4596.7	61
1.5	13.8	50	45	116200	561722	1994	360.8	1307.6	114
1.5	22.22	80	45	116200	561722	5108	921.9	3352.7	112
1.5	27.77	100	45	116200	561722	7983.4	1439	5241.9	111
1.5	13.8	50	60	119736	578842	2421	468.5	1128.2	124
1.5	22.22	80	60	119736	578842	6203.2	1196.2	2894.2	126
1.5	27.77	100	60	119736	578842	9696.5	1865.6	4526.2	126

Appendix G - Caravan 1.0 m Draw Bar Data Sheet

Table 30: Caravan 1.0m Draw Bar Data

DrawBar Length (m)	Wind Velocity (m/s)	Speed (km/h)	Wind Angle	Nodes	Elements	Force x (N)	Force y (N)	Force z (N)	Iter
1.0	13.8	50	0	111292	537382	517.2	59.4	11.1	99
1.0	22.22	80	0	111292	537382	1324	153.5	28.5	100
1.0	27.77	100	0	111292	537382	2068.9	241.4	44.6	100
1.0	13.8	50	15	112135	542228	850.1	72.9	617.5	82
1.0	22.22	80	15	112135	542228	2176.4	183.8	1584.9	82
1.0	27.77	100	15	112135	542228	3400.6	285.1	2479.1	82
1.0	13.8	50	30	112664	544693	1350.3	150.6	1082.6	65
1.0	22.22	80	30	112664	544693	3458.1	382.9	2776.9	65
1.0	27.77	100	30	112664	544693	5404.3	596.5	4342.6	65
1.0	13.8	50	45	114354	552521	1904	244.8	1234.6	87
1.0	22.22	80	45	114354	552521	4876.4	621.7	3163.4	87
1.0	27.77	100	45	114354	552521	7620.7	968	4944.5	87
1.0	13.8	50	60	116707	564604	2359.2	431.7	1096.9	109
1.0	22.22	80	60	116707	564604	6043.6	1097.9	2811.4	108
1.0	27.77	100	60	116707	564604	9445.7	1710.2	4395.2	107

Appendix H - Caravan 1.8m Draw Bar with Modified Edges

Table 31: Caravan 1.8m Draw Bar with Modified Edge Data

DrawBar Length (m)	Edge Curvature (mm)	Wind Velocity (m/s)	Speed (km/h)	Wind Angle	Nodes	Elements	Force x (N)	Force y (N)	Force z (N)	Iter
1.8m	100	13.8	50	0	126914	612651	494.3	89.2	15.9	122
1.8m	100	22.22	80	0	126914	612651	1265.6	230.4	40.5	119
1.8m	100	27.77	100	0	126914	612651	1977.6	361.4	63.4	118
1.8m	100	13.8	50	15	125279	605307	773.5	44.3	571.3	80
1.8m	100	22.22	80	15	125279	605307	1979.3	109.9	1464.6	80
1.8m	100	27.77	100	15	125279	605307	3092.1	169.5	2289.7	80
1.8m	100	13.8	50	30	126977	613238	1266.7	200.2	1075.9	75
1.8m	100	22.22	80	30	126977	613238	3242.1	513.1	2759.8	76
1.8m	100	27.77	100	30	126977	613238	5064.8	802.3	4315.2	76
1.8m	100	13.8	50	45	126186	609947	1876.2	258.3	1102.9	124
1.8m	100	22.22	80	45	126186	609947	4805.5	658.1	2827.8	128
1.8m	100	27.77	100	45	126186	609947	7509.6	1026.4	4420.9	129
1.8m	100	13.8	50	60	131071	632977	2231.3	466.9	912.6	79
1.8m	100	22.22	80	60	131071	632977	5713.9	1190.5	2339.3	80
1.8m	100	27.77	100	60	131071	632977	8929.6	1856.4	3657.5	81
1.8m	350	13.8	50	0	116626	563846	484.7	80.9	38.1	100
1.8m	350	22.22	80	0	116626	563846	1240.8	207.2	87.7	101
1.8m	350	27.77	100	0	116626	563846	1938.5	323.7	154.9	101
1.8m	350	13.8	50	15	116177	562091	731.2	99.9	529.2	73
1.8m	350	22.22	80	15	116177	562091	1871.6	254.2	1357.6	73
1.8m	350	27.77	100	15	116177	562091	2924.2	396.3	2123	73
1.8m	350	13.8	50	30	116915	565292	1185.6	197.1	1036.5	66
1.8m	350	22.22	80	30	116915	565292	3035.2	501.5	2657.6	66
1.8m	350	27.77	100	30	116915	565292	4742.6	781.5	4155.4	66
1.8m	350	13.8	50	45	119243	576405	1646.4	336.4	1219.8	70
1.8m	350	22.22	80	45	119243	576405	4216.5	858.8	3127.7	70
1.8m	350	27.77	100	45	119243	576405	6590.6	1337.5	4891.3	71
1.8m	350	13.8	50	60	121870	589494	2031.9	446.2	938.2	95
1.8m	350	22.22	80	60	121870	589494	5202.1	1133.1	2406.5	96
1.8m	350	27.77	100	60	121870	589494	8131.3	1764.4	3764.3	97

Appendix I - Caravan 1.5m Draw Bar with Modified Edges

Table 32: Caravan 1.5m Draw Bar with Modified Edge Data

DrawBar Length (m)	Edge Curvature (mm)	Wind Velocity (m/s)	Speed (km/h)	Wind Angle	Nodes	Elements	Force x (N)	Force y (N)	Force z (N)	Iter
1.5m	100	13.8	50	0	136777	659412	1296.7	230.1	4.7	91
1.5m	100	22.22	80	0	136777	659412	1294.3	228.9	4.6	89
1.5m	100	27.77	100	0	136777	659412	2021.5	358	7.2	90
1.5m	100	13.8	50	15	137118	660991	764.7	79.4	564.1	83
1.5m	100	22.22	80	15	137118	660991	1956.4	196	1445.5	84
1.5m	100	27.77	100	15	137118	660991	3056.3	301	2259.7	85
1.5m	100	13.8	50	30	136501	657094	1229.7	228.1	1031.5	59
1.5m	100	22.22	80	30	136501	657094	3146	583.2	2643.5	59
1.5m	100	27.77	100	30	136501	657094	4914.4	910.6	4132.3	59
1.5m	100	13.8	50	45	137502	661822	1752.7	135.1	1130	101
1.5m	100	22.22	80	45	137502	661822	4487.5	338.6	2896.1	101
1.5m	100	27.77	100	45	137502	661822	7012.1	524.1	4528.1	101
1.5m	100	13.8	50	60	143920	692787	2150.5	495.9	894.2	103
1.5m	100	22.22	80	60	143920	692787	5509	1260.2	2285.1	111
1.5m	100	27.77	100	60	143920	692787	8609.1	1960.4	2567.5	112
1.5m	350	13.8	50	0	124556	600292	491.6	108.2	-3	99
1.5m	350	22.22	80	0	124556	600292	1257	277.2	-8	98
1.5m	350	27.77	100	0	124556	600292	1963.1	432.5	-14	97
1.5m	350	13.8	50	15	124604	599442	717.1	132.2	505.6	100
1.5m	350	22.22	80	15	124604	599442	1834.7	331.8	1297.2	100
1.5m	350	27.77	100	15	124604	599442	2865.9	514.3	2029	99
1.5m	350	13.8	50	30	125430	603880	1124	237.4	965.9	66
1.5m	350	22.22	80	30	125430	603880	2876.9	604.4	2477.4	66
1.5m	350	27.77	100	30	125430	603880	4494.9	942.2	3874.1	66
1.5m	350	13.8	50	45	125430	603880	1124	237.4	965.9	66
1.5m	350	22.22	80	45	125430	603880	2876.9	604.4	2477.4	66
1.5m	350	27.77	100	45	125430	603880	4494.9	942.2	3874.1	66
1.5m	350	13.8	50	60	129267	623763	1832.8	486.7	839.2	80
1.5m	350	22.22	80	60	129267	623763	4689.7	1237.6	2147.4	80
1.5m	350	27.77	100	60	129267	623763	7323.3	1927.9	3354.6	80

Appendix J - Caravan 1.0m Draw Bar with Modified Edges

Table 33: Caravan 1.0m Draw Bar with Modified Edge Data

DrawBar Length (m)	Edge Curvature (mm)	Wind Velocity (m/s)	Speed (km/h)	Wind Angle	Nodes	Elements	Force x (N)	Force y (N)	Force z (N)	Iter
1.0m	100	13.8	50	0	126205	609042	471.7	108	2.4	90
1.0m	100	22.22	80	0	126205	609042	1206.3	278.7	6.3	92
1.0m	100	27.77	100	0	126205	609042	1883.5	436.2	10.1	94
1.0m	100	13.8	50	15	125735	607314	745.7	114.8	551.4	89
1.0m	100	22.22	80	15	125735	607314	1907.4	292.3	1412.6	89
1.0m	100	27.77	100	15	125735	607314	2979.3	456	2207.8	88
1.0m	100	13.8	50	30	125917	608641	1198.9	235.7	1018.3	67
1.0m	100	22.22	80	30	125917	608641	3067.9	605.9	2612	68
1.0m	100	27.77	100	30	125917	608641	4792.6	948.2	4084.5	68
1.0m	100	13.8	50	45	128518	620711	1697.4	127.6	1151.6	73
1.0m	100	22.22	80	45	128518	620711	4345.8	323.2	2953.5	72
1.0m	100	27.77	100	45	128518	620711	6791	501.6	4618.7	72
1.0m	100	13.8	50	60	131019	632689	2093.1	521	923.6	80
1.0m	100	22.22	80	60	131019	632689	5359.6	1329.6	2365.2	82
1.0m	100	27.77	100	60	131019	632689	8375.1	2075	3697.5	82
1.0m	350	13.8	50	0	116350	561171	452.8	111.7	-1	96
1.0m	350	22.22	80	0	116350	561171	1158.6	288.2	-2.8	97
1.0m	350	27.77	100	0	116350	561171	1809.6	451.3	-4.5	98
1.0m	350	13.8	50	15	116232	561045	732.8	242.1	487.1	98
1.0m	350	22.22	80	15	116323	561045	1817.1	492.3	1293.8	97
1.0m	350	27.77	100	15	116323	561045	2837.9	768.3	2022.3	98
1.0m	350	13.8	50	30	117432	567697	1104.7	275.8	944.8	61
1.0m	350	22.22	80	30	117432	567697	2827.3	705	2422	61
1.0m	350	27.77	100	30	117432	567697	4417.3	1110.7	3787.6	61
1.0m	350	13.8	50	45	118239	570695	1524.1	315.7	1135.4	108
1.0m	350	22.22	80	45	118239	570695	3902.6	804.8	2910.3	109
1.0m	350	27.77	100	45	118239	570695	6098.7	1255.4	4550.1	110
1.0m	350	13.8	50	60	121066	584538	1924.2	636	1067.9	83
1.0m	350	22.22	80	60	121066	584538	4929.7	1628	2738.5	83
1.0m	350	27.77	100	60	121066	584538	7705.1	2543.7	4282.2	83

Appendix K - Baseline Caravan with Frontal Vane System

Table 34: Frontal Vane System Data

| Wind Angle	Nodes	Elements	Force x (N)	Force y (N)	Force z (N)	Convergence Iterations
0	127913	616718	1170.4	199.6	-35.9	84
15	128041	617914	1789.4	222.3	1427.7	111
30	129411	625684	2891.4	547.6	2526.1	66
45	130492	630090	3966.6	268.3	2851.3	89
60	133744	645976	5124	909	2127.7	102
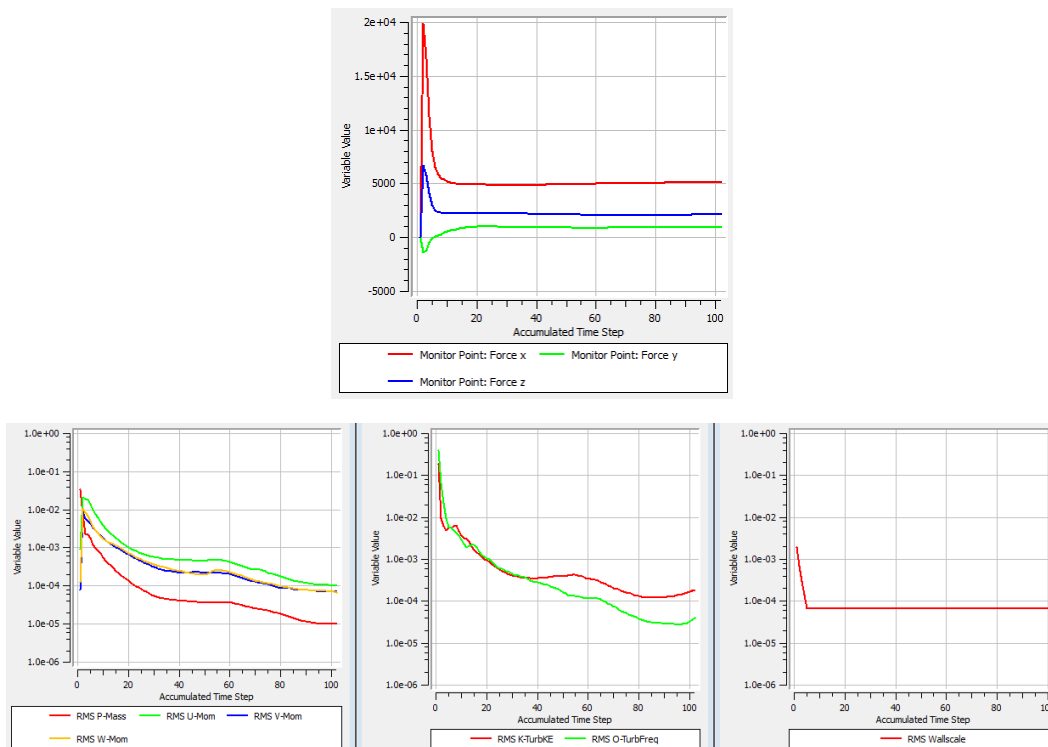
Figure K1: Residuals for Final Caravan Model with Vanes